2014

Rollover, drowning, and discontinuous retreat: Distinct modes of barrier response to sea-level rise arising from a simple morphodynamic model

Jorge Lorenzo Trueba
Montclair State University, lorenzotruej@mail.montclair.edu

Andrew Dale Ashton
Woods Hole Oceanographic Institution, aashton@whoi.edu

Published Citation

Lorenzo-Trueba, J., & Ashton, A. D. (2014). Rollover, drowning, and discontinuous retreat: Distinct modes of barrier response to sea-level rise arising from a simple morphodynamic model. Journal of Geophysical Research-Earth Surface, 119(4), 779-801. doi:10.1002/2013jf002941

AGU PUBLICATIONS

JGR

Journal of Geophysical Research: Earth Surface

RESEARCH ARTICLE
10.1002/2013JF002941

Key Points:
- Results highlight the importance of using a morphodynamic modeling approach
- Internal dynamics lead to more complex behaviors than previously suggested
- Time lags in the shoreface response to barrier overwash lead to periodic retreat

Supporting Information:
- Readme
- Dynamic equilibrium
- Height drowning
- Width drowning
- Discontinuous retreat
- Texts S1–S3

Correspondence to:
J. Lorenzo-Trueba,
jorge@whoi.edu

Citation:
Lorenzo-Trueba, J., and A. D. Ashton (2014), Rollover, drowning, and discontinuous retreat: Distinct modes of barrier response to sea-level rise arising from a simple morphodynamic model, *J. Geophys. Res. Earth Surf.*, *119*, doi:10.1002/2013JF002941.

Received 2 AUG 2013
Accepted 4 MAR 2014
Accepted article online 13 MAR 2013

Rollover, drowning, and discontinuous retreat: Distinct modes of barrier response to sea-level rise arising from a simple morphodynamic model

Jorge Lorenzo-Trueba[1] and Andrew D. Ashton[1]

[1]Geology and Geophysics Department, Woods Hole Oceanographic Institution, Woods Hole, Massachusetts, USA

Abstract We construct a simple morphodynamic model to investigate the long-term dynamic evolution of a coastal barrier system experiencing sea-level rise. Using a simplified barrier geometry, the model includes a dynamic shoreface profile that can be out of equilibrium and explicitly treats barrier sediment overwash as a flux. With barrier behavior primarily controlled by the maximum potential overwash flux and the rate of shoreface response, the modeled barrier system demonstrates four primary behaviors: height drowning, width drowning, constant landward retreat, and a periodic retreat. Height drowning occurs when overwash fluxes are insufficient to maintain the landward migration rate required to keep pace with sea-level rise. On the other hand, width drowning occurs when the shoreface response rate is insufficient to maintain the barrier geometry during overwash-driven landward migration. During periodic barrier retreat, the barrier experiences oscillating periods of rapid overwash followed by periods of relative stability as the shoreface resteepens. This periodic retreat, which occurs even with a constant sea-level rise rate, arises when overwash rates and shoreface response rates are large and of similar magnitude. We explore the occurrence of these behaviors across a wide range of parameter values and find that in addition to the maximum overwash flux and the shoreface response rate, barrier response can be particularly sensitive to the sea-level rise rate and back-barrier lagoon slope. Overall, our findings contrast with previous research which has primarily associated complex barrier behavior with changes in external forcing such as sea-level rise rate, sediment supply, or back-barrier geometry.

1. Introduction

Coastal barriers (barrier islands and spits) are long, thin, low-lying, sandy stretches of land, typically oriented subparallel to the mainland coast [*Reinson*, 1979; *Heward*, 1981]. Occupying ~7% of modern coasts [*Stutz and Pilkey*, 2001], barriers are vital landforms that not only host ecological resources and infrastructure; they often protect inland population centers and coastal ecosystems from storm damage [*Stone and McBride*, 1998; *Valdemoro et al.*, 2007; *FitzGerald et al.*, 2008]. Barriers face, however, an unknown future over the coming centuries as already rising sea levels are predicted to significantly accelerate [*Rahmstorf et al.*, 2012].

Higher sea levels will inundate low-lying coastal barriers, leaving them more susceptible to flooding and damage from storms. The flooding hazards associated with passive inundation can be reasonably estimated using high-quality topographic data [*González et al.*, 2005]. However, coastal barriers do not behave as a "bathtub"—increased sea levels enhance the ability for waves to reorganize the coast, typically resulting in increased shoreline retreat by moving sediment either offshore into deeper waters or onshore by overwashing the existing coast [*Leatherman*, 1983; *Donnelly et al.*, 2006]. The projected rates of sea-level rise over the next century far exceed those experienced over the past several millennia [*IPCC*, 2007], and the potential exists for historically unprecedented changes and increases in hazards, including the possibility for a total loss of protective natural barriers. Thus, a main objective of this work is to explore the threshold mechanisms of morphologic barrier response to sea-level rise. To directly address the question, we construct a simple morphodynamic model for barrier evolution.

2. Background

Barrier islands are not static landforms (Figure 1), they are dynamic, with waves constantly reworking and moving sediment back and forth over a wide range of temporal and spatial scales. The long-term evolution of coastal barriers is the result of the complex interplay of the different regions or environments.

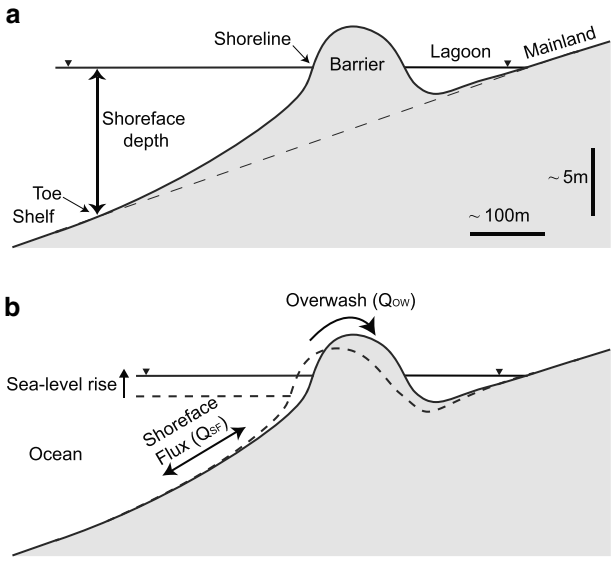

Figure 1. Typical cross section of a barrier system demonstrating (a) key components and (b) the process domains. Note the strong exaggeration of the vertical scale (vertical and horizontal scale bars are included).

Considering long-term evolution (decades to centuries, to millennia), the characteristic environments found within a typical barrier system, from ocean to mainland, are the continental shelf, offshore of the barrier system; the shoreface, the submerged profile reworked by waves; the subaerial region, including the beach and coastal dunes; and the back-barrier environment, which typically includes marshes and a lagoon or a bay. These environments are separated by three main geomorphic boundaries: the shoreface toe, which separates the continental shelf and the shoreface; the shoreline, which separates the shoreface or marine system from the subaerial region; and the back-barrier, which separates the barrier system from the preexisting back-barrier topography. These internal moving boundaries can be tracked as part of the solution to an overall morphological evolution problem [*Swenson et al.*, 2000; *Lorenzo-Trueba et al.*, 2009; *Lorenzo-Trueba and Voller*, 2010]. To first order, here we assume that the primary controls on the cross-shore evolution of these moving boundaries are the changes in sea level, shoreface dynamics, and storm overwash.

2.1. Barriers and Sea-Level Rise History

Modern barrier islands, which originated in the Holocene thousands of years ago as sea-level rise decelerated, occur worldwide yet are predominantly found along passive margin coasts [*FitzGerald et al.*, 2008; *Stutz and Pilkey*, 2011; *McBride et al.,* 2013]. The mechanisms of barrier island formation continue to be debated, with several hypotheses proposed, from submergence of alongshore-extending spits to sand bar emergence [*De Beaumont*, 1845; *Gilbert*, 1885; *McGee*, 1891; *Hoyt and Henry*, 1971; *Otvos*, 1985]. Regardless of the formation mechanism, substantial evidence demonstrates that many barrier systems have migrated landward over the last few thousand years through overwash processes, maintaining themselves even as the sea level slowly rose [*Leatherman*, 1979; *McBride et al.,* 2013]. For instance, along the Atlantic coast of the United States, barrier complexes likely formed as global sea-level rise slowed to less than 10 mm/yr at the end of the early Holocene, approximately 7000 years ago [*Engelhart et al.*, 2009; *Thieler and Ashton*, 2011], and have been transgressing landward since. Offshore of modern barrier complexes of New Jersey and New York, geologic evidence suggests that in the early Holocene, barriers existed many kilometers seaward of their current position [*Stuiver and Daddario*, 1963; *Stahl et al.*, 1974; *Rampino and Sanders*, 1980].

In most cases, barrier islands retreat with sea-level rise, but there are some exceptions. First, there are cases in which the barrier system is not able to keep up with sea level and eventually drowns [*Sanders and Kumar*, 1975; *Nummedal et al.*, 1984; *FitzGerald et al.*, 2008; *Mellett et al.*, 2012]. Second, there are cases in which a high sediment input, either from offshore or alongshore sources, can offset the tendency to retreat. More specifically, when the rate of sediment input exceeds the rate of accommodation created by sea-level rise, the shoreline progrades seaward [*Scheinerman*, 1996]. This was the case of Galveston Island ~3000 years ago as it migrated over fluvial deposits, which served as a sand source, and enabled the barrier to regress even as sea level rose [*Rodriguez et al.*, 2004]. Another example can be found in the Dutch coast, where riverine sediment input during the Holocene lead to the stabilization and local progradation of barriers in the southern coast, while the northern coast continued its retreat until today [*Beets and Van der Spek*, 2000]. In this manuscript, we focus on the retreat and drowning of barriers with closed sediment budgets; future studies will address external input of sediments.

2.2. The Shoreface and Sea-Level Rise

The shoreface is the active littoral region in which sediment is primarily transported by waves. Typically concave-upward [*Dean*, 1991], the shoreface extends offshore to a depth where waves have marginal effect and sediment transport becomes exceedingly low in comparison to regions higher in the shoreface. The shoreface toe, or closure depth, is thus the limit to significant morphologic evolution [*Hallermeier*, 1981; *Nicholls et al.*, 1998]; accordingly, the closure depth is a function of not only wave conditions but also the timescale of interest [*Stive et al.*, 1991; *Wright et al.*, 1991; *Stive and de Vriend*, 1995; *Wright*, 1995].

It has been long understood that due to the presence of an active shoreface, the response of a wave-affected coast to sea-level rise is more complex than inundation alone. This concept underlies the Bruun rule [*Bruun,* 1962, 1988], which predicts shoreline change due to sea-level rise based upon conservation of mass and the assumption of maintenance of an equilibrium shoreface shape. Despite being widely applied by the engineering and scientific communities, there remains considerable debate regarding Bruun rule [*Cowell et al.*, 1995; *Wolinsky and Murray*, 2009]. For instance, there are varying definitions of the appropriate closure depth. On the one hand, the engineering community typically determines the depth of closure based on changes at annual to decadal timescales [e.g., *Hallermeier*, 1981], whereas coastal geologists often consider a deeper closure depth that is more appropriate for centennial and millennial time scales.

The Bruun rule also assumes that the shoreface maintains an equilibrium geometric configuration, and thus, its response to sea-level rise is instantaneous or, more generally, much faster than the rate of sea-level rise itself. However, the shoreface is a transitional region, with slower dynamics in lower regions, and thus prone to out-of-equilibrium states. Some possible perturbations of the equilibrium shoreface shape include the extraction of sediment from the upper shoreface during storms [*Donnelly et al.*, 2006], gradients in alongshore sediment transport [*Stive et al.*, 2002; *Ashton and Murray*, 2006], and beach nourishment [*Smith et al.*, 2009]. The concept that shoreface evolution, at least in terms of the lower portions of the active shoreface, may be slower than instantaneous [*Stive and de Vriend*, 1995] will be a focus of our investigation.

2.3. Barrier Overwash

In order for barrier systems to persist and migrate landward during a period of sea-level rise, nearshore sediment must be transported onto and behind the barrier (Figure 1b). Storm-induced inlet and flood-tidal delta formation and overwash fan deposition are the two most significant mechanisms of transporting sediment to the back-barrier environment [*Dillon*, 1970; *Pierce*, 1970; *Fitzgerald et al.*, 1984; *Donnelly et al.*, 2006]. Although overwash occurs during punctuated storm events, these individual events accumulate to represent a long-term and exclusively landward sediment flux. *Leatherman* [1979] introduces the concept of a "critical barrier width," which suggests that overwash tends to be slow until a barrier narrows. When the barrier narrows, overwash becomes frequent and the barrier enters a rollover phase. Note that within this framework, overwash is considered the landward movement of sand by barrier overtopping, inundation, or even the temporary opening of inlets.

Recent modeling studies have started to incorporate overwash transport of sediments [*Donnelly et al.*, 2006]. For instance, the concept of critical barrier width has been numerically implemented into long-term models of barrier and shoreline evolution [*Jiménez and Sánchez-Arcilla*, 2004; *Ashton and Murray*, 2006; *Masetti et al.*, 2008; *McNamara and Werner*, 2008]. Other models of barrier overwash tend to focus on the short-term fluxes from single events [*Larson et al.*, 2004; *Donnelly et al.*, 2006]; these short-term events are integrated over time in the model presented by *Rosati et al.* [2010]. The recently developed X-Beach model [*Roelvink et al.*, 2009], which simulates barrier overtopping and erosion by resolving infragravity-timescale processes, has been applied to reproduce barrier changes by individual storm events [*Lindemer et al.*, 2010; *McCall et al.*, 2010]. However, computation of overwash-driven changes using high-resolution models such as X-Beach over timescales of barrier evolution (decades to centuries) by integrating over multiple storm events and including post-storm recovery and fair weather action remains unexplored to our knowledge.

2.4. Previous Approaches to Modeling Barrier Evolution

Traditionally, understanding of the profile response of barriers to sea-level rise has relied upon geometric relationships, such as modifications to the Bruun rule [*Dean and Maurmeyer*, 1983; *Ranasinghe and Stive*, 2009; *Ranasinghe et al.*, 2012]. *Wolinsky and Murray* [2009] provide a generalized analytic approach to the modified Bruun rule, demonstrating that long-term trajectories of barriers are controlled by the inland topography, not

the shoreface slope as suggested by the Bruun rule. A numerical application of the modified Bruun rule, the Shoreline Translation Model (STM) model [*Cowell et al.*, 1995], computes the evolution of barrier systems over geological timescales by conserving mass and assuming the barrier maintains its geometry as sea level changes. This approach, also used by the GEOMBEST model [*Stolper et al.*, 2005; *Moore et al.*, 2010], allows more detailed treatment of sediment budgets and interactions with back-barrier geometries and lithologies. These models could be considered "morphokinematic" in that they advect geometries without specific concern to process, whether it be rates of overwash or out-of-equilibrium shoreface configurations.

Other model approaches allow relaxation of out-of-equilibrium geometries. Over short timescales, these approaches have been used to understand beach (and sometimes upper shoreface) response to changing wave conditions [*Larson and Kraus*, 1989; *Miller and Dean*, 2004; *Yates et al.*, 2009], using a supposition that the beach relaxes to a presumed equilibrium position at a rate proportional to the distance to the equilibrium position. Over longer timescales, a similar approach is implemented for barrier evolution in the GEOMBEST model [*Stolper et al.*, 2005; *Moore et al.*, 2010]. The general applicability of a distance-based disequilibrium relaxation to the long-term evolution of barrier landforms is perhaps less obvious. As overwash rates (and therefore information on the barrier geometry) affect the direction of shoreface fluxes, applying distance-based relaxation suggests that the marine domain (shoreface) has instantaneous knowledge of the configuration of terrestrial domain (and its effect on overwash). Overall, we consider these models based on distance from an equilibrium location to represent a type of "relaxed" morphokinematics.

In contrast, other numerical modeling approaches are more specifically "morphodynamic," in that they focus on sediment fluxes through feedback between the coupling of offshore and overwash dynamics. For instance, *Storms et al.* [2002], *Storms* [2003], and *Storms and Swift* [2003] use a "process-response" framework to investigate the impact of high energy events on the evolution and stratigraphic deposits of barriers. This model accounts for sediments of multiple sizes and, within the "process-response" framework, considers shoreface erosion and deposition as separate processes. Another example was developed by *Masetti et al.* [2008], who simulate the evolution of Holocene barriers along the Florida coast using a numerical model with dynamic shelf, shoreface, and overwash processes.

Another approach to forecasting future barrier vulnerability to storms and sea-level rise are Bayesian Networks [*Gutierrez et al.*, 2011; *Plant and Stockdon*, 2012]. Bayesian Networks have proven to be a useful approach for evaluating uncertainty and sensitivity to input parameters in predictions. However, this approach requires large amounts of observational data—such data may span sufficiently long timescales to represent long-term barrier change.

2.5. Objective and Structure

The key objective of this work is to introduce a simple morphodynamic model of barrier evolution that investigates potential modes of barrier behavior as a function of a wide swath of system parameters. In section 3, we develop a set of equations to describe the movement of the domain boundaries linked morphodynamically through process connections (Figure 1b). In section 4, we introduce a steady state analytical solution, and a more general numerical solution, for the system equations. In section 5, we present and discuss one model run for each mode of barrier response under constant sea-level rise. Section 6 explores the parameter space through regime diagrams, with a particular focus on the maximum rate of overwash and the shoreface response rate. We then discuss the results in terms of existing models of barrier evolution. Finally, in section 7, we describe in more detail some model features and discuss possible future research directions.

3. Model Description

3.1. Modeling Approach

The exploratory model [*Murray*, 2003] we present addresses barrier evolution with a goal of reducing the number of variables and processes. Our model focuses on two primary barrier components, or behavioral elements: the marine domain represented by the active shoreface and the terrestrial system, where the infrequent process of overwash controls landward mass fluxes (Figure 1b). These two systems both tend to change dramatically during storms and, similarly, are slowly active in-between. However, other than the

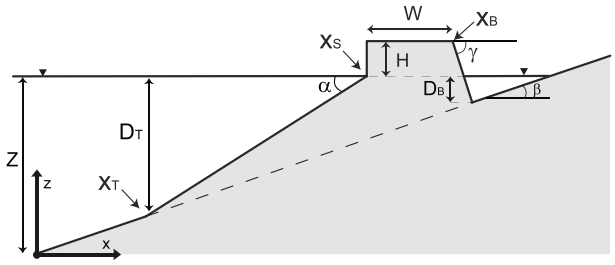

Figure 2. Barrier model setup and components.

coupling at the shared boundary of the shoreline, the dynamics and processes of these two systems are largely independent of one another.

3.2. General Model Setup

Similar to previous models for sedimentary basin evolution [*Swenson et al.*, 2000; *Lorenzo-Trueba et al.*, 2009; *Lorenzo-Trueba and Voller*, 2010; *Lorenzo-Trueba et al.*, 2012; *Lorenzo-Trueba et al.*, 2013], the key point of our approach is to consider a cross section through an idealized geometric configuration (Figure 2). Three main geomorphic boundaries define the system: the shoreface toe, the shoreline, and the top of the back-barrier face.

We define the origin at the shoreface toe at $t = 0$, with x positive landward and z positive upward. The shoreface toe is located at $x = x_T$ and $z = Z(t) - D_T$, where D_T is the depth of the shoreface toe and $Z(t)$ is the mean sea-level elevation. At $t = 0$, the elevation of the sea level is $Z(0) = D_T$. The shoreline is located at $x = x_S$ and $z = Z(t)$, and the top of the back-barrier face is located at $x = x_B$ and $z = Z(t) + H(t)$. We consider a back-barrier face with a fixed slope γ (note that as this slope γ has a modest effect on barrier behavior and is generally steeper than that of other subaqueous components, the calculations here assume a vertical back-barrier face). The subaerial portion of the barrier system, delimited by the shoreline and the back-barrier, is characterized by its width W and height above sea level H. A vertical profile for the exposed beach is reasonable as this slope is typically steep (~1–10°) compared to the shelf or the shoreface slopes [*Heward*, 1981]. The bathymetric profile landward of the subaerial barrier is characterized to first order by its maximum depth below sea level D_B and its mean slope β. Here we explore the case of a barrier superimposed upon a simple linear shelf/back-barrier slope; future versions of the model could easily be adapted to explore the role of more complex back-barrier configurations.

As opposed to previous morphodynamic models that spatially discretize the shoreface morphology, evolving its shape based on local sediment flux balances [*Storms et al.*, 2002; *Masetti et al.*, 2008; *Ashton and Ortiz*, 2011], we collapse the entire shoreface into a linear unit with slope α. We adopt this linear geometric approach for two reasons: (1) the linear slope typically approximates slope-driven transport models satisfactorily [*Kim and Muto*, 2007; *Lorenzo-Trueba and Voller*, 2010] and (2) the calculations are significantly simplified. We recognize, however, that there might be scenarios in which shoreface curvature changes become important and the linear approximation breaks down [*Lorenzo-Trueba et al.*, 2013]. More complex shoreface configurations might also be needed to account for offshore lithologic control; again for simplicity, the cases explored here assume that the shoreface is comprised of compatible noncohesive sediment.

For the simplified geometry considered in Figure 2, the shoreface slope α and the barrier width W can be expressed as

$$\alpha = D_T/(x_S - x_T), \tag{1}$$

and

$$W = x_B - x_S. \tag{2}$$

Additionally, for the particular case of a constant back-barrier lagoon slope β, the back-barrier depth D_B is defined geometrically as

$$D_B = Z - \beta x_B. \tag{3}$$

Provided an initial geometric configuration and the required input parameters, the evolution of the system can be fully determined with the rates of migration of the shoreface toe $\dot{x}_T = \mathrm{d}x_T/\mathrm{d}t$, the shoreline $\dot{x}_S = \mathrm{d}x_S/\mathrm{d}t$, the back-barrier $\dot{x}_B = \mathrm{d}x_B/\mathrm{d}t$, and the rate of change of the barrier height $\dot{H} = \mathrm{d}H/\mathrm{d}t$ over time. In the next section, we write these rates in terms of the leading processes behind the evolution of the barrier system: (1) shoreface fluxes, (2) passive flooding during sea-level rise, and (3) overwash. These three components are then incorporated into a complete morphodynamic model.

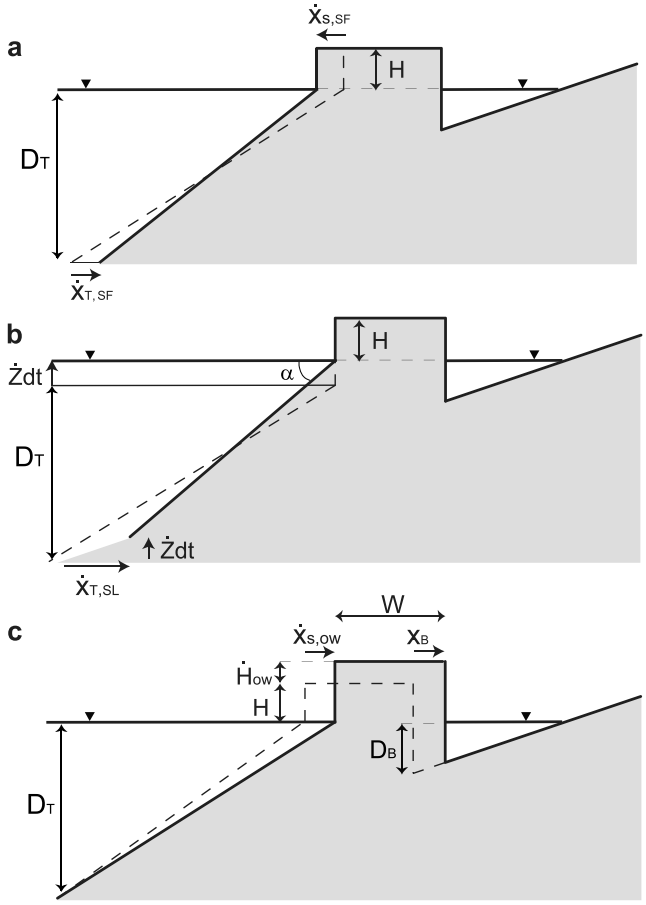

Figure 3. The three components of modeled barrier behavior: (a) shoreface sediment fluxes, (b) passive flooding during sea-level rise, and (c) barrier sediment exchange during overwash.

3.3. Shoreface Fluxes

Shoreface sediment fluxes are determined based upon deviations from an equilibrium profile (Figure 3a). This assumption is in keeping with previous mechanistic approaches to shoreface evolution whereby an equilibrium shoreface develops with onshore sediment transport by waves (asymmetry and drift) balanced by an offshore-directed gravity slope term [*Bowen*, 1980; *Bailard*, 1981; *Stive and de Vriend*, 1995]. Expanding upon these efforts and those of *Ortiz and Ashton* [2013] (see supporting information Text S1), Q_{SF} can be estimated by deviations of the shoreface slope α from an equilibrium slope α_e as follows:

$$Q_{SF} = K(\alpha_e - \alpha), \tag{4}$$

where K represents the shoreface flux rate constant ($m^3/m/s$). In Appendix S1, we present expressions for K and α_e under the assumption of both Airy wave theory and shallow water waves; in both cases K and α_e are functions of the wave period, wave height, settling velocity, and the local water depth z. In the model presented here, however, we assume that the shoreface is characterized by depth-integrated values of K and α_e.

Stive and de Vriend [1995] similarly demonstrate that the leading term for fluxes due to perturbations around an equilibrium are proportional to the slope, and similar relationships have been used for surf-zone processes [*Falqués et al.*, 1999]. Note that as K becomes very large, the shoreface responds rapidly such that the shoreface response collapses toward the Bruun rule, or "mophokinematic" behavior. Overall, our approach (and reasoning) behind the computation of out-of-equilibrium shoreface response differs from that of "relaxed morphokinematic" models in that we assume no equilibrium location and instead compute long-term sediment transport balances. Applying one response rate K to the entire shoreface is also a simplification, as the upper shoreface will respond significantly faster than the lower shoreface. Our approach, therefore, conceptualizes sediment exchange from the slower-responding lower shoreface with the shoreline.

Combining mass conservation with the geometric template presented in Figure 3a, we can quantify the shoreface response as

$$\dot{x}_{S,SF} = -4Q_{SF}\frac{H + D_T}{(2H + D_T)^2}, \tag{5}$$

and

$$\dot{x}_{T,SF} = 4Q_{SF}\frac{H + D_T}{D_T(2H + D_T)}. \tag{6}$$

3.4. Passive Flooding by Sea-Level Rise

The instantaneous effect of sea-level rise (i.e., neglecting sediment transport processes and overwash fluxes) is flooding, or passive inundation, which, for a concave shoreface, results in reduction of the barrier

height, translation of the barrier toe, and shoreface steepening [*Bruun*, 1962]. Representing these effects within our linear shoreface profile somewhat confounds this representation. However, moving the shoreline up the beach and translating the shoreface toe up the shoreface slope captures passive shoreface steepening. Assuming that the barrier sediment volume is maintained through the translation of these moving boundaries (see Figure 3b) leads to the following rates of change for the toe and the height:

$$\dot{x}_{T,\mathrm{SL}} = \frac{2\dot{z}}{\alpha}, \tag{7}$$

and

$$\dot{H}_{\mathrm{SL}} = -\dot{z}, \tag{8}$$

where the subindex *SL* stands for the sea-level-driven system response.

Again, this inundation process represents steepening that then drives offshore transport through a Bruun-type response (which is captured in the shoreface fluxes component of our model). This implementation suggests an onshore-directed sediment flux (Figure 3b), which is not exactly the case as this apparent flux is a geometric manifestation of the translation of the system boundaries. We attempted other implementations of this drowning response within the model and they did not affect model behavior—most vital is that sea-level rise causes oversteepening and that mass is conserved.

3.5. Overwash

The process of overwash removes sediment from the seaward portion of the barrier and deposits it landward [*Donnelly et al.*, 2006]. Here we first present the general framework for the movement of the domain boundaries for a given overwash flux. Next, we present an approach to computing long-term overwash fluxes based upon a back-barrier deficit volume concept. We use this approach in the model results presented here, but note that the general model framework is flexible such that it could also incorporate different approaches to computing overwash fluxes.

3.5.1. Overwash Fluxes

Although details of the depth of marine sediment excavation by overwash remain poorly understood, the sediment contributing to overwash is generally excavated from the beach, surf zone, and upper portions of the shoreface [*Hawkes and Horton*, 2012]. The simplest way to capture the overwash process with our basic model geometry is by assuming that overwash erosion takes place in the upper shoreface and beach, with the maximum erosion at the shoreline and zero erosion at the shoreface toe (Figure 3c). In this way, for a given sediment volume eroded per unit width and time Q_{OW}, we can compute the shoreline retreat rate as

$$\dot{x}_{S,\mathrm{OW}} = \frac{2Q_{\mathrm{OW}}}{D_T + 2H}. \tag{9}$$

Overwash sediment deposition can be separated into top-barrier $Q_{\mathrm{OW},H}$ and back-barrier $Q_{\mathrm{OW},B}$ components, i.e.,

$$Q_{\mathrm{OW}} = Q_{\mathrm{OW},B} + Q_{\mathrm{OW},H}. \tag{10}$$

Thus, overwash deposition onto the top-barrier $Q_{\mathrm{OW},H} > 0$ results in an increase in subaerial barrier elevation, and overwash deposition onto the back-barrier $Q_{\mathrm{OW},B} > 0$ leads to landward extension. The associated movements of the boundaries (Figure 3c) are

$$\dot{H}_{\mathrm{OW}} = \frac{Q_{\mathrm{OW},H}}{W}, \tag{11}$$

and

$$\dot{x}_{B,\mathrm{OW}} = \frac{Q_{\mathrm{OW},B}}{H + D_B}. \tag{12}$$

Note that equations (11) and (12) are general and can be applied for any computed quantities of overwash flux. Below, we present a method of overwash partitioning based on a "deficit volume concept," which we use in the solutions presented here.

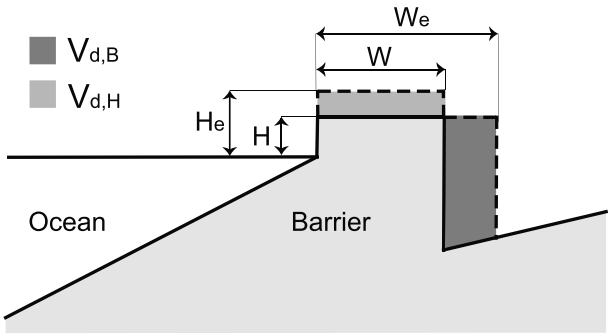

Figure 4. Schematic of the critical barrier island width concept and the top-barrier $V_{d,H}$ and back-barrier $V_{d,B}$ deficit volumes.

3.5.2. Barrier Deficit Volume Concept

As an extension of the general concept of a critical, or "equilibrium" barrier width W_e and commensurate equilibrium barrier height H_e, we define a "barrier deficit volume" V_d, which represents the difference, from a given shoreline location, between a current barrier configuration and one that is both high and wide enough such overwash is presumed not to occur. This volume per unit width (m^3/m), akin to the concept of accommodation (defined as the space made available for potential sediment accumulation), can have both top-barrier $V_{d,H}$ and back-barrier $V_{d,B}$ components (Figure 4). $V_{d,H}$ grows with the passive drowning of the barrier itself, whereas $V_{d,B}$ increases with a reduction in barrier width and is dynamically affected by changes in the shoreline location itself. The deficit volume components can then be computed as

$$V_{d,B} = \max[0, (W_e - W)(H + D_B)], \tag{13}$$

and

$$V_{d,H} = \max[0, (H_e - H)W], \tag{14}$$

where

$$V_d = V_{d,B} + V_{d,H}. \tag{15}$$

There is an overlap region in the deficit volume that could be designated as either top-barrier or back-barrier components (Figure 4). However, this designation becomes unimportant as the back-barrier volume deficit is generally an order of magnitude larger than the top-barrier deficit volume. Thus, for simplicity, we choose not to include this overlap region in the deficit volume.

The concept that more back-barrier accommodation than top-barrier accommodation is created by sea-level rise (which is often obscured by the vertical exaggeration of profile views, e.g., Figures 1–5) can be demonstrated using a simple dimensional argument. Assuming a sea-level rise of $\Delta Z = 1$ m, a barrier width of

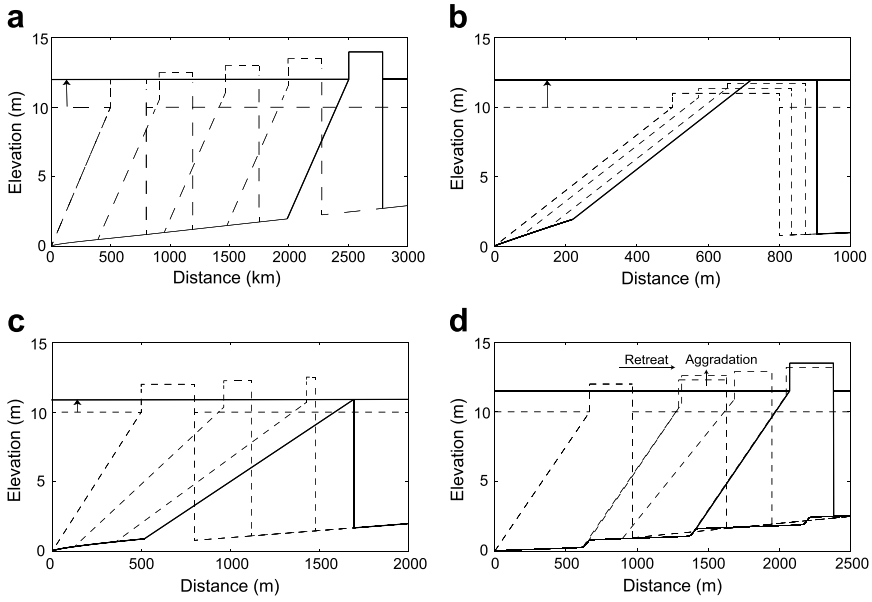

Figure 5. Profile evolution of modeled barrier systems response demonstrating (a) dynamic equilibrium, (b) height drowning, (c) width drowning, and (d) periodic periodic retreat. Input parameter values are included in Table 3.

$W = 100$ m, a back-barrier vertical elevation of ~ 2 m, and a back-barrier lagoon slope $\beta = 10^{-3}$, the top-barrier accommodation is $V_{d,H} = 100\ m^3/m$. To estimate $V_{d,B}$, we assume that the barrier geometry is maintained during landward migration as in morphokinematic models [*Cowell et al.*, 1995; *Wolinsky and Murray*, 2009], which leads to a landward barrier translation of $\Delta Z/\beta = 1000$ m. The associated back-barrier accommodation with such a landward migration is $V_{d,B} = 2000\ m^3/m$, more than an order of magnitude larger than the top-barrier accommodation. It follows that the low aspect ratios of barriers mean that sea-level rise induces effective accommodation growth preferentially in the back-barrier (rather than top-barrier, i.e., $V_{d,B} >>> V_{d,H}$).

The presence of a barrier deficit volume does not indicate that a barrier is unstable to sea-level rise. On the contrary, the concept of a critical barrier width assumes that such a deficit drives overwash, which could potentially result in steady state barrier rollover.

3.5.3. Partitioning of the Overwash Flux

We use a simplified relationship to compute barrier overwash, which extends upon the barrier deficit concept described above [*Leatherman*, 1983]. We partition the total overwash flux into back-barrier and top-barrier components, and each component is assumed to scale with their respective deficit volumes. We also assume that there exists a maximum rate of potential barrier overwash $Q_{OW,max}$ and a commensurate maximum deficit volume $V_{d,max}$. The overwash fluxes are thus computed as

$$Q_{OW,B} = Q_{OW,max} \frac{V_{d,B}}{\max\left(V_d, V_{d,max}\right)}, \tag{16}$$

and

$$Q_{OW,H} = Q_{OW,max} \frac{V_{d,H}}{\max\left(V_d, V_{d,max}\right)}, \tag{17}$$

where

$$Q_{OW} = Q_{OW,B} + Q_{OW,H}. \tag{18}$$

In this way, the total overwash Q_{OW} is set to the maximum value $Q_{OW,max}$ for barrier deficits greater than $V_{d,max}$. In Appendix S3, we explore the sensitivity to these parameters and find that variations in $V_{d,max}$ have a minor effect on barrier behavior, whereas as demonstrated in the results below, $Q_{OW,max}$ plays a major role.

Site-specific estimates of $Q_{OW,max}$ are similarly difficult to make, but this flux should depend upon storm frequency and magnitude as well as local sediment characteristics. However, because this parameter represents a maximum flux, it is unlikely that a given barrier will be currently overwashing at this rate, particularly if the barrier in question is not currently in a rollover state. A compilation of measured overwash volumes from individual events compiled by *Carruthers et al.* [2013] suggests single-storm overwash fluxes generally range in the order of 10 to up to $190\ m^3/m$. However, given the infrequency of storm strikes, these fluxes should be convolved with storm frequency to estimate a longer-term flux. *Carruthers et al.* [2013] present a potential approach for estimating long-term overwash fluxes using overwash from a known event. Estimating the width-averaged volume of a specific overwash deposit caused by a known major storm V_{OW}, and the recurrence interval R_{OW} (estimated through the analysis of meteorological, tide gauge, or other proximal data), provides a general estimate of potential long-term for the overwash flux: $Q_{OW} = V_{OW}/R_{OW}$.

Although the deficit volume approach vastly oversimplifies the complex process of barrier overwash [*Donnelly et al.*, 2006; *Roelvink*, 2006; *Roelvink et al.*, 2009; *McCall et al.*, 2010], particularly as sufficiently large storms may still cause overwash, our approach bears resemblance to approaches used in other models [*Jiménez and Sánchez-Arcilla*, 2004; *Masetti et al.*, 2008; *McNamara and Werner*, 2008]. More importantly, it encapsulates the sensible concept that low and skinny barriers are more prone to overwash. As we state above, the profile-averaged approach also allows our parameterization to encompass breaching and temporary inlet formation. For this reason, we include the back-barrier depth in the deficit calculation as sediment deposition from breaching processes can depend on the back-barrier accommodation.

4. Model Solution

The evolution of the barrier system is fully determined by the rates of change of the shoreface toe $\dot{x}_T$, shoreline $\dot{x}_S$, back-barrier $\dot{x}_B$, and height $\dot{H}$. Combining the shoreface response (*SF*), passive flooding

during sea-level rise (*SL*), and the barrier overwash (*OW*) components we obtain the following expressions:

$$\dot{x}_T = 4Q_{SF}\frac{H + D_T}{D_T(2H + D_T)} + \frac{2\dot{z}}{\alpha}, \tag{19}$$

$$\dot{x}_S = \frac{2Q_{OW}}{2H + D_T} - 4Q_{SF}\frac{H + D_T}{(2H + D_T)^2}, \tag{20}$$

$$\dot{x}_B = \frac{Q_{OW,B}}{H + D_B}, \tag{21}$$

and

$$\dot{H} = \frac{Q_{OW,H}}{W} - \dot{z}, \tag{22}$$

where the overwash sediment fluxes $Q_{OW,B}$ and $Q_{OW,H}$ are calculated from equations (13) to (18) and the shoreface sediment flux Q_{SF} from equation (4).

4.1. Dynamic Equilibrium

For a given sea-level rise rate $\dot{z}$, a steady state solution exists for equations (19) to (22) in which the rate of change of the subaerial portion of the barrier is zero $\dot{H} = 0$, and the rate of landward barrier translation equals that of all three barrier boundaries: $\dot{x}_T = \dot{x}_S = \dot{x}_B = \dot{z}/\beta$. Substituting these rates into equations (21) and (22), we obtain the width W_{de} and height H_{de} at dynamic equilibrium:

$$W_{de} = W_e - \frac{\dot{z}}{\beta}\frac{V_{d,max}}{Q_{OW,max}}, \tag{23}$$

and

$$H_{de} = H_e - \dot{z}\frac{V_{d,max}}{Q_{OW,max}} \tag{24}$$

If sea level is constant (i.e., $\dot{z} = 0$), then the barrier system is in static equilibrium (i.e., $W = W_e$, $H = H_e$, and $\alpha = \alpha_e$). When $\dot{z} > 0$, however, W_{de} and H_{de} are smaller than the critical values (i.e., $W_{de} < W_e$, $H_{de} < H_e$), which allows an overwash flux to be maintained. Combining equations (20) and (17), we obtain the shoreface slope at dynamic equilibrium:

$$\alpha_{de} = \frac{\xi\alpha_e - \dot{z} + \sqrt{(\xi\alpha_e - \dot{z})^2 + 8\beta\xi\dot{z}}}{2\xi}, \tag{25}$$

where

$$\xi = \frac{4\beta K}{D_T}\left(\frac{H_{de} + D_T}{2H_{de} + D_T}\right). \tag{26}$$

When $\dot{z} > 0$, the value α_{de} is also below critical (i.e., $\alpha_{de} < \alpha_e$), which leads to a net onshore sediment flux at the shoreface computed as $Q_{SF,de} = K(\alpha_e - \alpha_{de})$. This highlights an important consequence of a morphodynamic approach: for a barrier to be in dynamic equilibrium with sea-level rise, the net shoreface fluxes must be directed onshore, a phenomenon that would seem to contradict the general principle of shoreface oversteepening that underlies the Bruun response. The solution here, however, demonstrates that an onshore-directed shoreface flux is parsimonious with the dynamic equilibrium shoreface concept—for the case of a rollover barrier, overwash flattens the shoreface driving onshore fluxes whereas in the absence of overwash, shoreface oversteepening by sea-level rise drives an offshore-directed shoreface flux.

Additionally, using the equations above and after some algebra we can write the overwash flux at dynamic equilibrium $Q_{OW,de}$ as follows:

$$Q_{OW,de} = \frac{\dot{z}}{\beta}\left(H_{de} + D_{B,de}\right) + \dot{z}W_{de}, \tag{27}$$

where

$$D_{B,de} = D_T(1 - \beta/\alpha_{de}) + \beta W_{de}. \tag{28}$$

Table 1. State Variables and their Dimensions

Symbol	Meaning	Dimensions (L, length, T time)
α	shoreface slope	-
D_B	back-barrier depth	L
H	barrier height	L
Q_{OW}	overwash sediment flux	-
$Q_{OW,H}$	overwash sediment flux to the top-barrier	L^2/T
$Q_{OW,B}$	overwash sediment flux to the back-barrier	L^2/T
Q_{SF}	shoreface sediment flux	L^2/T
t	Time	T
V_d	deficit volume per unit width	L^2
$V_{d,H}$	top-barrier deficit volume per unit width	L^2
$V_{d,B}$	back-barrier deficit volume per unit width	L^2
W	barrier width	L
x	horizontal distance (positive landward)	L
x_S	shoreline position	L
$\dot{x}_s$	rate of change of shoreline position	L/T
x_T	shoreface toe position	L
$\dot{x}_T$	rate of change of shoreface toe position	L/T
x_B	back-barrier face position	L
z	vertical distance positive upward	L
Z	sea level	L

4.2. Numerical Solution

To examine coupled, nonsteady state behavior, we numerically solve equations (13) to (22) at a given time $t > 0$ by computing the positions of each boundary x_T, x_S, x_B, and the height H at a small increment of time Δt using a simple Euler scheme $\xi = \xi^{\text{old}} + \dot{\xi}\Delta t$, where $\xi = x_T,\ x_S,\ x_B,\ H$. All of the variables and input parameters involved in the calculation are included in Tables 1 and 2. In Table 3, we include all the input parameter values used in the calculations in sections below. As initial geometry, we choose

$$\alpha(t=0) = \alpha_e, W(t=0) = W_e, \text{and } Z(t=0) = D_T. \tag{29}$$

This initial geometry is at static equilibrium (i.e., $\dot{x}_T = \dot{x}_S = \dot{x}_B = \dot{H} = 0$) for a constant sea level (with corresponding zero shoreface and overwash fluxes).

5. Modeled Barrier Behaviors

Below we describe the behaviors of the system for a given constant sea-level rise rate $\dot{z}$ and a constant back-barrier lagoon slope β.

5.1. Dynamic Equilibrium

At dynamic equilibrium, overwash and shoreface fluxes are sufficiently high and equivalent to maintain the geometric configuration of the barrier during landward migration (Figures 5a and 6). Initially, the geometry is

Table 2. Description and Typical Values of the Input Parameters[a]

Symbol	Meaning	Typical value range
D_T	depth of the shoreface toe	10-20 m
z	relative sea-level rise rate	0-10 mm/y
β	back-barrier lagoon slope	$10^{-5} - 10^{-3}$
W_e	critical barrier width	~0.1-1 km
H_e	critical barrier height the top-barrier	~0.5-3 m
α_e	shoreface slope at static equilibrium	0.01-0.02
K	shoreface response rate	0-10,000 m^3/m/y
$Q_{OW,\max}$	maximum overwash sediment flux	0-100 m^3/m/y
$V_{d,\max}$	maximum deficit volume	$0 \le V_{d,\max} \le H_e W_e$

[a]Most parameters are poorly constrained and site specific, particularly K and $Q_{OW,\max}$. Note that the sea-level rise rate $\dot{z}$ includes both local sea-level rise and subsidence rates.

Table 3. Input Parameters Used in Figures 5–12, 14, and 15

Figure	$K(m^3/m/y)$	$Q_{OW,max}(m^3/m/y)$	$V_{d,max}(m^3/m)$	$\alpha_e(-)$	$\beta(-)$	W_e (m)	H_e (m)	D_T (m)	$\dot{z}$(mm/y)
5a and 6	10,000	40	300	0.02	0.001	300	2	10	2
5b and 7	10,000	5	100	0.02	0.001	300	1	10	7
5c and 8	1,000	80	100	0.02	0.001	300	2	10	7
5d and 9	10,000	100	100	0.015	0.001	300	2	10	3
10	*varies*	*varies*	100	0.02	0.001	300	2	10	2
11	*varies*	*varies*	100	0.02	0.001	300	2	10	*varies*
12	*varies*	*varies*	100	0.02	*varies*	300	2	10	2
14a	2,000	*varies*	100	0.02	0.001	300	2	10	*varies*
14b	4,000	*varies*	100	0.02	*varies*	300	2	10	2
15	*varies*	*varies*	200	0.015	0.001	300	1	15	3

at static equilibrium as defined in equation (29). Perhaps many modern barriers may be in a similar static condition after experiencing relatively stable sea level for the last several millennia. As the sea level rises, overwash fluxes are activated, which results in shoreface flattening and barrier narrowing. In turn, as the barrier narrows, the overwash fluxes increase; this positive feedback between overwash fluxes and barrier geometry leads to a short-lived decrease in barrier width and shoreface slope below their values at dynamic equilibrium (i.e., $W < W_{de}$ and $\alpha < \alpha_{de}$). When the onshore sediment fluxes at the shoreface are large enough to restore the barrier width, the barrier geometry asymptotically decays to the dynamic equilibrium configuration. This "overshoot" arises from the dynamic model and the initial assumption of a static barrier; however, as we detail below, long-term behavior depends on system parameters, not the initial conditions. This morphodynamic response contrasts with geometric relaxation shown by other models due to a change in back-barrier shape from an initially out-of-equilibrium condition [*Wolinsky and Murray*, 2009].

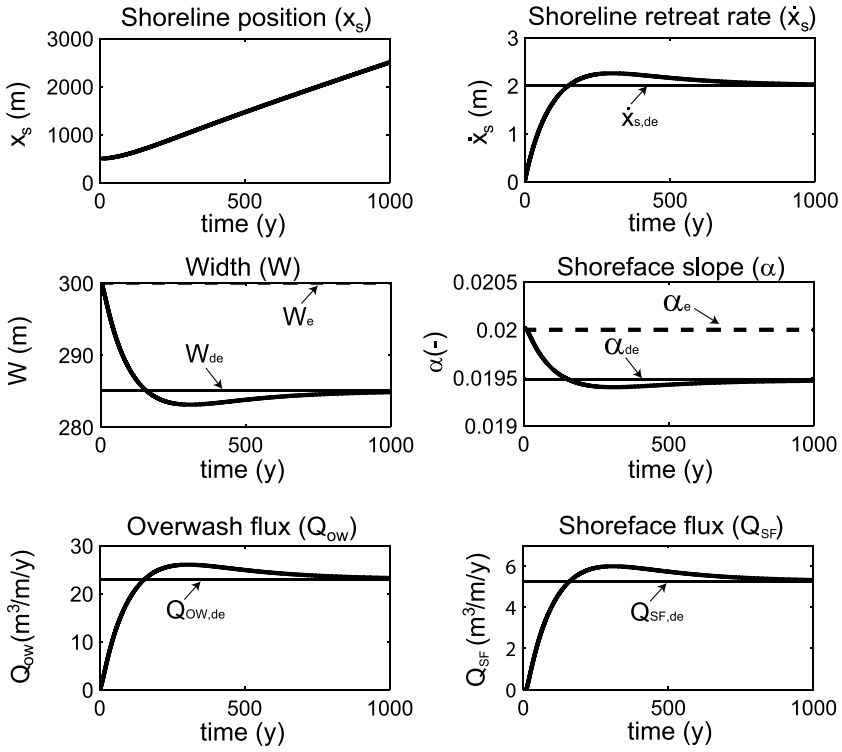

Figure 6. Time evolution of key variables for a barrier system that attains dynamic equilibrium. The input parameter values are the same as in Figure 6a and are included in Table 3. The values at dynamic equilibrium are calculated using equations (22)–(27).

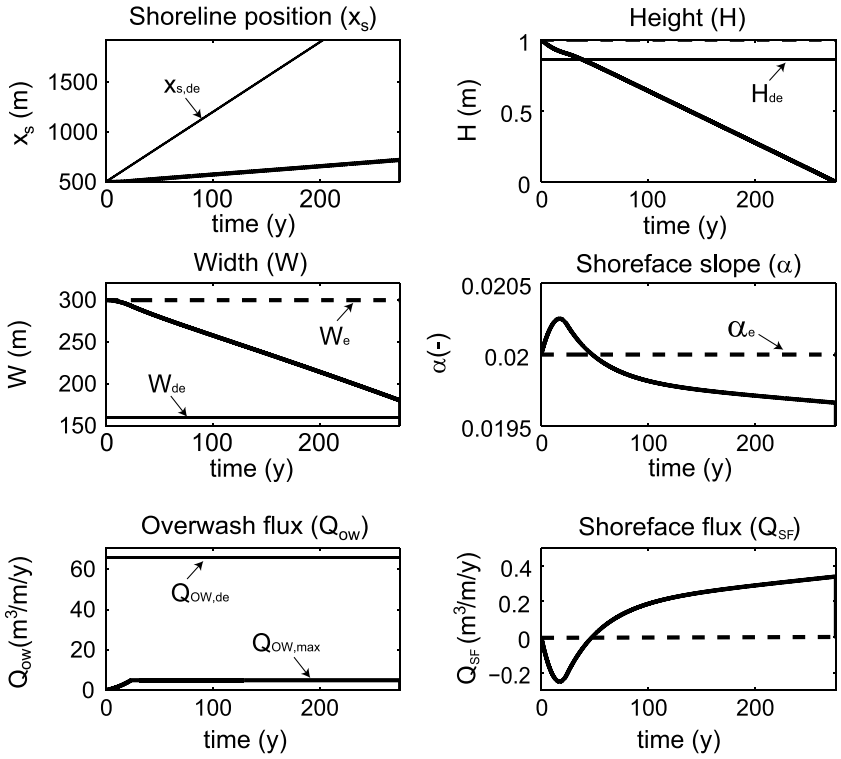

Figure 7. Time evolution of key variables for a barrier system that undergoes "height drowning." The input parameter values are the same as in Figure 6b and are included in Table 3.

5.2. Barrier Drowning

Modeled barriers are not always able to keep pace with sea-level rise; we identify two modes of barrier drowning: height drowning and width drowning.

5.2.1. Height Drowning

When overwash fluxes are insufficient to maintain the landward migration rate required to keep pace with sea-level rise, the barrier drowns even though it has maintained a sufficient width, a phenomenon we term "height drowning." In this case, limited overwash flux results in the shoreline migrating slower than the rate required for dynamic equilibrium (Figures 5b and 7), similar to the drowning response demonstrated by *Fagherazzi et al.* [2003] and *Storms et al.* [2008]. Consequently, barrier height undergoes a continuous decay, with the barrier eventually drowning (i.e., $H < 0$). Here we use "height drowning" in a general sense to represent a barrier that drowns due to insufficient overwash fluxes. In a natural setting, it may be difficult to ascertain the difference between "height" and "width" drowning from local observations.

5.2.2. Width Drowning

Large overwash fluxes can result in a different mode of barrier collapse. When the shoreface response rate is low such that onshore sediment transport is insufficient to maintain the barrier geometry during landward migration, a barrier experiences what we term "width drowning." In this case, the rate of shoreline migration significantly exceeds that of dynamic equilibrium (Figures 5c and 8), and consequently, the width undergoes a rapid decay and eventually disintegrates (i.e., $W < 0$). This novel result demonstrates that high rates of barrier overwash do not necessarily allow a barrier to survive sea-level rise.

5.3. Periodic Retreat

When the barrier system does not drown, it does not necessarily (and often does not) attain a constant landward migration rate. Even with constant forcing, the coupled overwash-shoreface system can undergo periodic retreat. This periodic response is characterized by oscillations of the state variables around the dynamic equilibrium (Figure 9). The amplitude of the oscillations is maintained over geological time scales

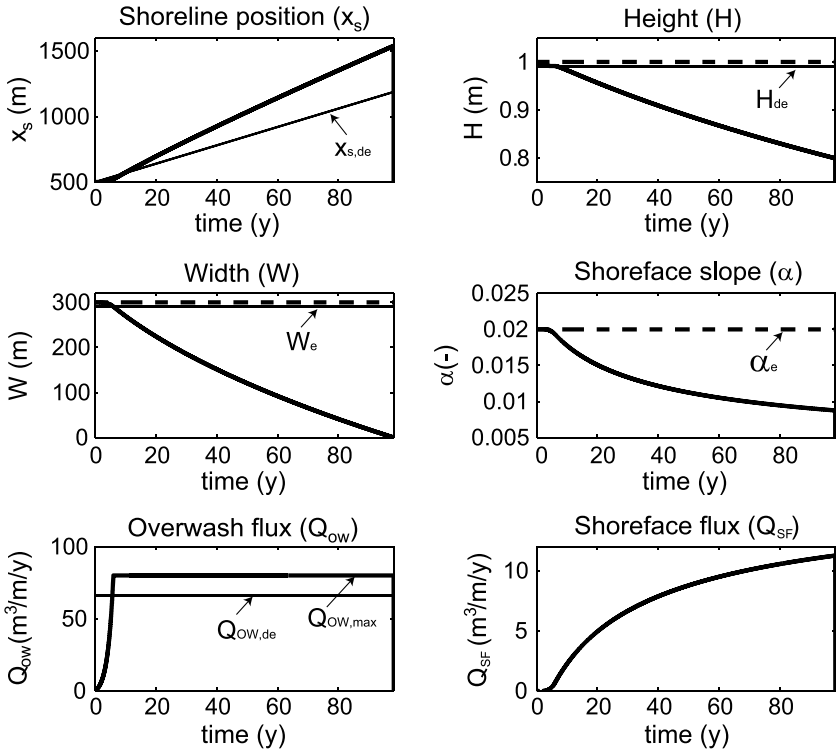

Figure 8. Time evolution of key variables for a barrier system undergoing "width drowning." The input parameter values are the same as in Figure 6c and are included in Table 3.

and occurs when $Q_{OW,max}$ is high enough to allow a rapid landward migration of the barrier and K is high enough to avoid width drowning.

The periodic behavior begins with the barrier undergoing rapid transgression and experiencing large rates of overwash. Onshore fluxes from the shoreface toe cannot compensate for the overwash fluxes, and the barrier narrows as the shoreface flattens further from its equilibrium (Figures 6d and 9). Eventually, the shoreface slope becomes sufficiently flat that increased onshore sediment fluxes start to increase the barrier width (even as the barrier shoreline is transgressing). Eventually, the barrier widens to its critical value and overwash fluxes to the back-barrier shut down. Consequently, the barrier stops its landward migration and an aggradational phase begins. However, the shoreface fluxes are still directed onshore, and with no overwash occurring, barrier width rapidly increases until the shoreface slope returns to its equilibrium configuration—at this point the width reaches a maximum. As the sea level continues to rise, the shoreline retreats and the barrier width slowly decreases. As overwash is inactive, shoreface fluxes are directed offshore and the shoreline retreat is consistent with a Bruun-rule-type behavior. Eventually the width decreases below its critical value—a threshold is crossed—and the overwash fluxes take over again and a new transgressive phase, characterized by significantly more rapid shoreline retreat, begins.

The alternation between the transgressive and aggradational phases repeats periodically, maintaining the amplitude and frequency of the oscillations. This oscillatory behavior arises from time lags in the shoreface response to overwash, and thus, the amplitude and length of the width oscillations increase as the shoreface response rate K decreases (Figure 10). Both the amplitude and the length also increase as the maximum overwash flux rate $Q_{OW,max}$ increases. Overall, the amplitude and period of the oscillations are determined by system parameters and internal dynamics, and the characteristics of the long-term periodic behavior do not arise from the initial conditions of a static barrier configuration (see supporting information Text S2). In this case, dynamic equilibrium is an unsteady stable state of the system. Note also that during this periodic behavior, although the long-term rate of barrier retreat is controlled by the rate of sea-level rise and the back-barrier slope, as suggested by geometric models [*Wolinsky and Murray*, 2009], the barrier system temporarily experiences short-term retreat rates far in excess of the long-term rate prescribed by the back-barrier slope.

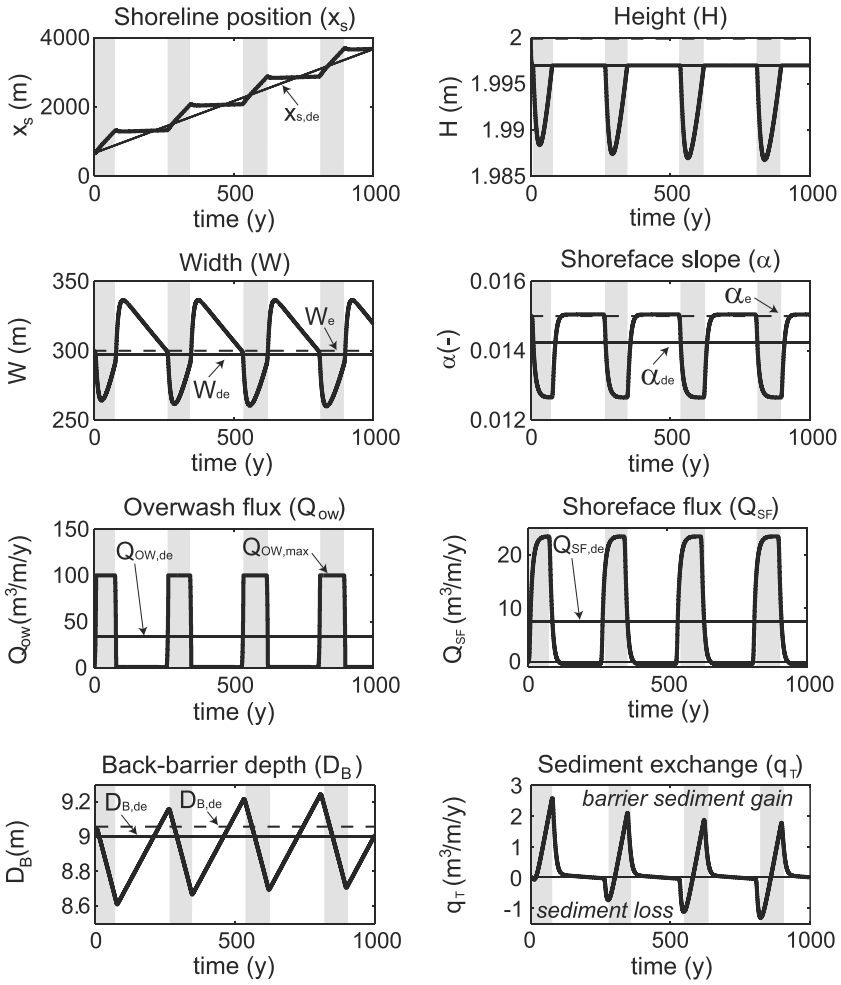

Figure 9. Time evolution of key variables for a barrier system undergoing "periodic periodic retreat." Shaded intervals correspond to transgressive intervals. The input parameter values are the same as in Figure 6d and are included in Table 3.

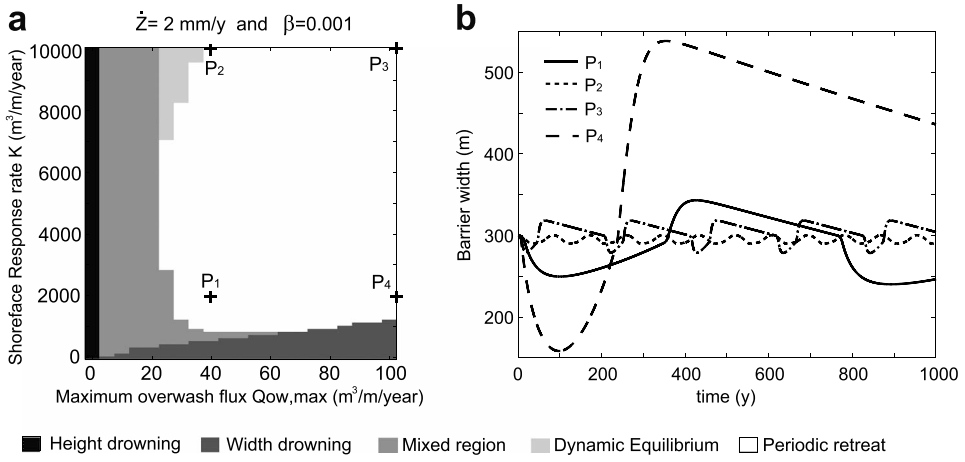

Figure 10. (a) Regime diagram including different system behaviors as shoreface response rate and maximum overwash flux are varied. (b) Barrier width over time for four different cases in the periodic retreat region as indicated. The input parameter values are included in Table 3.

6. Exploring The Parameter Space

The simplicity of the model allows us to explore barrier behavior across a wide range of parameter values. Because the coupled system behavior is strongly controlled by overwash and shoreface dynamics, we construct a series of "regime diagrams" as a function of the shoreface response rate K and the maximum overwash flux $Q_{OW,max}$. Supported by our calculations in supporting information Text S1, we explore K across the range $0 - 10,000$ m^2/yr. Based on compiled estimates of storm-driven overwash fluxes [*Carruthers et al.*, 2013], we explore the long-term overwash flux $Q_{OW,max}$ within the range $0 - 100$ m^2/yr. We further discuss methods to potentially estimate these parameters below in the discussion.

Spanning these ranges of values for K and $Q_{OW,max}$, the resulting regime diagrams include the four behaviors described in previous section (Figure 10). We identify the dynamic equilibrium when the barrier height, width, and shoreface slope reach and maintain their dynamic equilibrium values (see equations (23) to (26)). Height and width drowning are identified when the conditions $H < 0$ and $W < 0$ are met, respectively. Periodic retreat potentially could also be identified analytically as the system approaches a periodic orbit; however, an analytic approach is more simply applied to two-dimensional systems, becoming significantly more challenging for higher order systems such as the one we investigate [*Scheinerman*, 1996]. We use a simplified heuristic approach to our numerical solutions and identify periodic retreat using two conditions: (1) the mean amplitude of the barrier width oscillations must be higher than 1 m and (2) the amplitude of the width oscillations at any time must be within 80% of the mean amplitude (i.e., the amplitude is roughly maintained during the running time). The limited model running time (i.e., $T_{max} = 1000$ year) potentially interferes with this criteria. For instance, if the system oscillates with a period that is beyond the running time, the criteria will fail to identify any of the four behaviors. A similar problem arises when the time of drowning is longer than the running time. Thus, we group these atypical responses in what we define as the "mixed region" (Figure 10).

Overall, model explorations demonstrate that the sea-level rise rate $\dot{z}$ and the back-barrier lagoon slope β play a major role in the system response. Other input parameters, including $V_{d,max}$, D_T, W_e, H_e, and A_e, have a modest effect, as demonstrated in supporting information Text S3.

6.1. Sea-Level Rise Rate

As might be expected, barrier drowning is more likely for higher rates of sea-level rise $\dot{z}$ (Figure 11). Interestingly, an increase in $\dot{z}$ results in a larger expansion of the width drowning region than that experienced by the height drowning region. This rapid expansion of the width drowning occurs as larger sea-level rise rates $\dot{z}$ increase the overwash sediment flux required to keep pace with sea level $Q_{OW,de}$ (see equation (27)). To a lesser degree, larger values for the shoreface response rate K help to maintain intact barriers. Note also that the periodic response mode occupies a significant portion of the parameter space and appears to be favored over the development of dynamic equilibrium.

6.2. Back-Barrier Lagoon Slope

Barrier behavior is also sensitive to changes in the back-barrier lagoon slope β (Figure 12). In general, barrier drowning is more likely for flatter slopes (small β), as the barrier must migrate landward faster to keep pace with sea level. Intuitively, faster rates of overwash should facilitate such rapid migration. However, this rapid overwash can outstrip the onshore flux from the shoreface, eventually leading to width drowning. As a result, as β decreases the width drowning region expands rapidly to take over most of the parameter space (Figure 12).

Note the difference in the expansion of the width drowning regime for changes in $\dot{z}$ versus β (Figures 11 and 12)—whereas rapid overwash can preserve a barrier experiencing rapid sea-level rise, rapid overwash can also facilitate barrier drowning for flat back-barriers. Additionally, because of the increased overwash sediment flux required to keep pace with sea level as β decreases (see equation (27)), flatter back-barriers are less likely to experience dynamic equilibrium.

6.3. Comparison to Previous Modeling Efforts

With the exception of the dynamic equilibrium retreat, the behaviors exhibited by our simple model cannot be recreated by "morphokinematic" models based upon the conservation of mass and maintenance barrier geometry [*Cowell et al.*, 1995; *Wolinsky and Murray*, 2009]. Morphokinematic model predictions do not

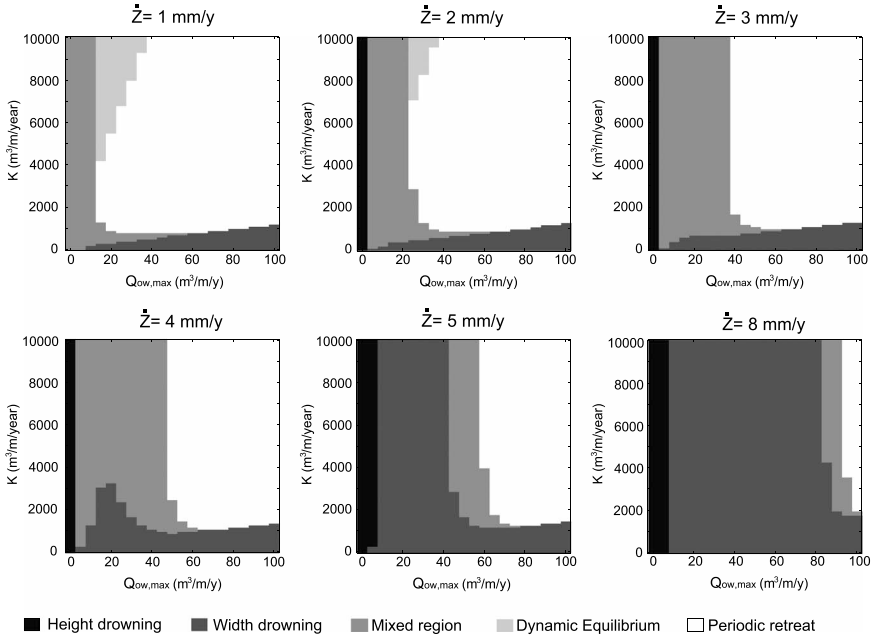

Figure 11. Regime diagrams as a function of the maximum overwash flux $Q_{OW,max}$ and the shoreface flux constant K for different values of the sea-level rise rate z. The back-barrier lagoon slope is $\beta = 0.001$. The other parameter values are included in Table 3.

depend on the rate of sea-level rise $\dot{z}$ but only on the magnitude of change of the sea level Δz, as if the barrier was always at dynamic equilibrium. However, the results presented above suggest that the region for dynamic equilibrium only represents a small portion of the parameter space. This implies that the dynamics of the coupled overwash shoreface system play a major role in the type of barrier response, driving behaviors such as drowning and periodic periodic retreat.

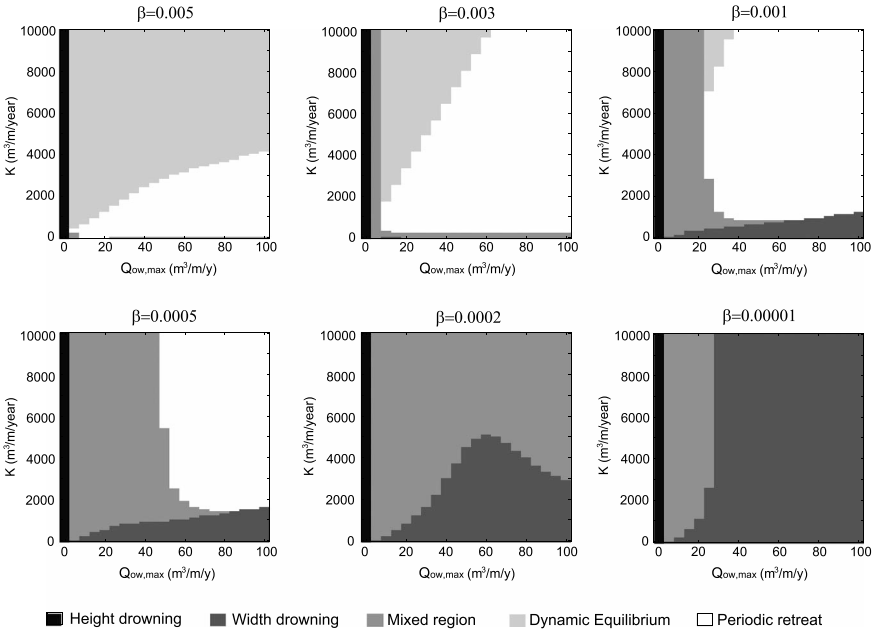

Figure 12. Regime diagrams as a function of the maximum overwash flux $Q_{OW,max}$ and the shoreface flux constant K for different values of the back-barrier lagoon slope β. The sea-level rise rate is $z = 0.002$. The other input parameter values are included in Table 3.

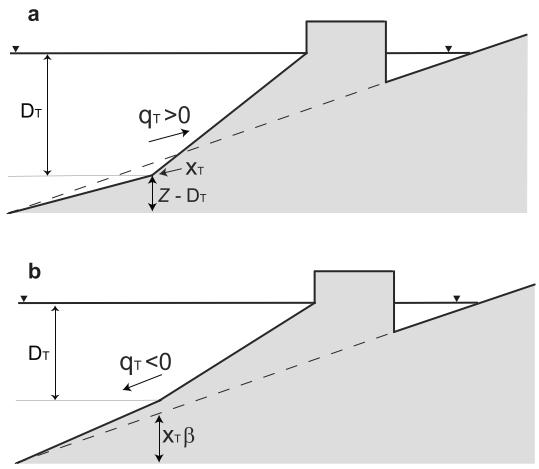

Figure 13. Sketches of sediment exchange between the shelf and the barrier. (a) Sediment import of sediments from the shelf to the barrier. (b) Sediment export from the barrier to the shelf.

Similarly, although "relaxed" morphokinematic models can result in barrier drowning, they only reproduce one type (height) drowning and certainly do not exhibit the periodic retreat mode. Furthermore, our morphodynamic system exhibits periodic retreat exactly when both shoreface response and overwash rates are high, assumptions that underlay morphokinematic approaches. Therefore, although "relaxed" morphokinematic models can shed much understanding in terms of recreating past sediment budgets [*Stolper et al.*, 2005; *Moore et al.*, 2010], the results presented here suggest that their general application may be appropriate only in limited cases.

The model presented here is not the first one to use a dynamic approach to modeling barrier evolution [*Storms et al.*, 2002; *Storms*, 2003; *Storms and Swift*, 2003; *Storms and Hampson*, 2005; *Masetti et al.*, 2008; *Storms et al.*, 2008] but is the first one to explore complex barrier dynamics (e.g., Figure 9) across a wide range of parameter values (Figures 10–12). Moreover, to the authors' knowledge the model is the first one to hypothesize that under constant forcing (i.e., $\dot{z} =$ constant) and no variations in the back-barrier configuration (i.e., $\beta =$ constant), a barrier system can undergo periodic oscillations around the dynamic equilibrium.

7. Discussion

In this section we discuss the sediment exchange between the barrier and the shelf produced by the model and the dependence of the time of drowning of barriers on the long-term overwash flux and the shoreface response rate. We also qualitatively compare the different model behaviors with observations and suggest approaches to estimate the key parameter values. Last, we discuss some important model limitations and future model developments.

7.1. Sediment Exchange Between the Barrier and the Shelf

The sediment exchange between the barrier and the shelf can result in important variations in barrier sediment volume as the system migrates landward. In the model presented, the sediment exchange flux q_T can be computed as the product between the rate of migration of the shoreface toe $\dot{x}_T$ and the toe elevation with respect to the basement h_T, i.e.,

$$q_T = -\dot{x}_T h_T \tag{30}$$

where the toe elevation is geometrically defined as $h_T = Z - D_T - \beta x_T$ (Figure 13). Under sea-level rise, the toe migration is always directed onshore (i.e., $\dot{x}_T > 0$). Thus, if the toe elevation is negative (i.e., $h_T < 0$), the toe excavates into the shelf and supplies the barrier system with additional sediment (i.e., $q_T > 0$), whereas a positive toe elevation $h_T > 0$ implies that the barrier is exporting sediments onto the shelf (i.e., $q_T < 0$).

The sea-level rise rate $\dot{z}$ and the back-barrier lagoon slope β are key controls of the barrier-shelf sediment exchange. Intuitively, as $\dot{z}$ increases or β flattens, it becomes more difficult for the barrier to incise into the shelf during landward migration (i.e., the barrier sediment loss to the shelf increases) (Figure 14).

The mode of barrier behavior also controls the sediment exchange pattern. At dynamic equilibrium, the shoreface toe elevation is always zero (i.e., $h_T = 0$), and thus, there is no sediment exchange between the barrier and the shelf (Figure 5a). Interestingly, however, during periodic retreat there is an alternation between barrier sediment gain and loss during landward migration (Figures 5d and 9). Note that this exchange is purely morphodynamic since it occurs in the absence of spatial changes of the back-barrier slope and therefore cannot be captured by "relaxed" morphokinematic models [*Stolper et al.*, 2005; *Moore et al.*,

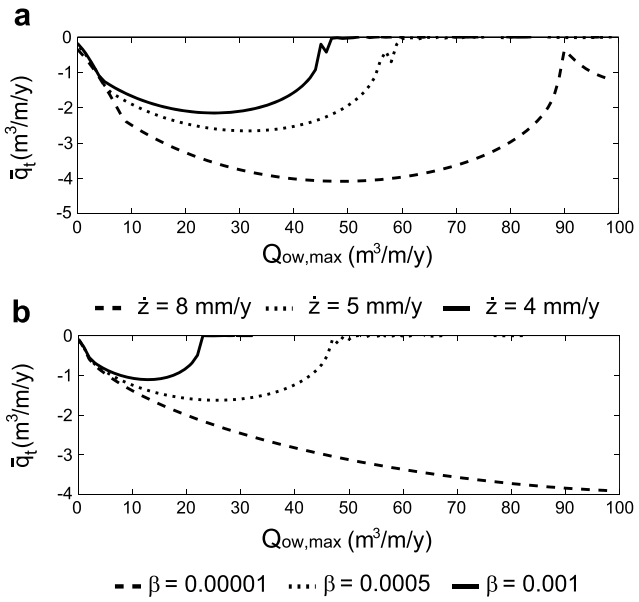

Figure 14. Average sediment loss to the shoreface toe as the barrier migrates landward (i.e., $\bar{q}_t < 0$) as a function of the maximum overwash flux $Q_{OW,max}$ for different (a) sea-level rise rates $\dot{z}$ and (b) back-barrier lagoon slopes β. Figure 14a includes three transects of three regime diagrams from Figure 11 for $K = 2000$ m^2/y, and Figure 14b includes transects of regime diagrams from Figure 12 for $K = 4000$ m^2/y.

2010]. Lastly, barrier drowning typically leads to barrier sediment loss to the shelf (Figures 5b and 5c). Further investigation of these interactions, however, would require a more explicit shoreface treatment as well as consideration of shoreface grain size variations.

7.2. Drowning Time

The drowning time of barriers is largely dependent on the rates of overwash. During height drowning, overwash fluxes limit the ability of the barrier to keep pace with sea level. Thus, the time of drowning increases as we increase the maximum overwash rate $Q_{OW,max}$ (Figure 15). Beyond a threshold value of $Q_{OW,max}$, however, the barrier fails via width drowning. Accordingly, the width drowning time also depends on the shoreface response rate K (Figure 15). Lower values of K reduce the ability of the barrier to maintain its geometric configuration during landward migration. For larger overwash fluxes, the landward migration rate increases, consequently reducing the time of width drowning. In contrast, for large values of K, the shoreface is able to maintain its configuration even under high rates of landward migration, and the time of drowning increases as we increase $Q_{OW,max}$. Interestingly, for intermediate K values, small changes in $Q_{OW,max}$ can lead to abrupt changes in the time of drowning (Figure 15) as the system is at the boundary between width drowning and periodic retreat.

Barrier drowning is also controlled by other factors such as the sea-level rise rate $\dot{z}$ and the back-barrier lagoon slope β. As discussed above, an increase in $\dot{z}$ or a reduction in β enhances barrier drowning (Figures 11 and 12).

7.3. Comparison to Natural Barriers

Again, the purpose of this exploratory model is to better understand potential barrier dynamics across a wide range of parameter space. The model simplicity somewhat hinders direct comparison to specific cases, although above we offer some techniques to estimate the key system parameters. Comparison to observed system behavior can help constrain whether the dynamics revealed by our model are reasonable.

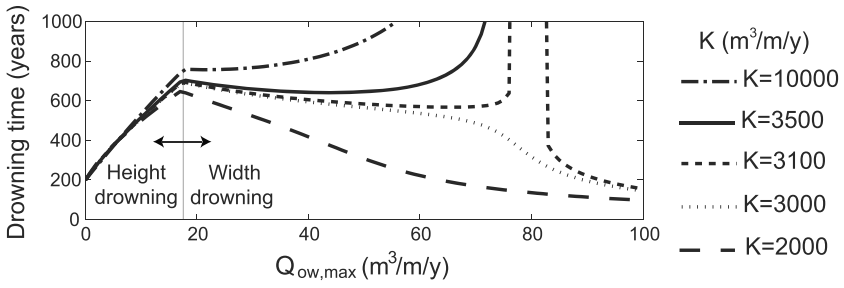

Figure 15. Time of drowning during barrier landward migration as a function of the maximum overwash $Q_{OW,max}$. Input parameter values are included in Table 3.

Geologic observations demonstrate that many barrier systems worldwide have been able to keep pace with sea-level rise for thousands of years [*McBride et al.,* 2013]. There are differences, however, in the nature of the migration of different barriers. In some cases, geologic evidence suggests landward barrier retreat through continuous migration (rollover) and complete reworking of the barrier deposits offshore [*Swift*, 1975; *Swift and Moslow*, 1982], much like the dynamic equilibrium mode in the model. Attaining such dynamic equilibrium after a sudden change in the sea-level rise rate might require thousands of years according to both model results and field observations [*Daley and Cowell*, 2012]. In particular, model results demonstrate that a sudden rise in the sea-level rise can take on the order of thousand years to reach dynamic equilibrium (Figure 6).

Other studies suggest barriers may have undergone periodic retreat and episodic overstepping, leading to the alternation of preserved remnants of barrier deposits and erosional surfaces [*Rampino and Sanders*, 1980; *Forbes et al.*, 1991; *Mellett et al.*, 2012]. Often such episodic retreat is attributed to variations in external forcing such as sea-level rise rate [*Clifton*, 2006; *Mellett et al.*, 2012], sediment input [*Clifton*, 2006; *Mellett et al.*, 2012], and tidal amplitude [*Storms et al.*, 2008]. Here, however, we show that the intrinsic complexity of the system, and in particular feedback between shoreface and overwash processes, can also lead to periodic episodes of shoreline retreat under constant sea-level rise.

Barrier deposits are unlikely to be preserved as they are transgressed, accordingly, their remains scant evidence of drowned barriers on continental shelves [*Mellett et al.*, 2012]. The interpretation of shelf sand bodies, however, has allowed coastal geologists to hypothesize the occurrence of two types of barrier drowning. In-place drowning [*Sanders and Kumar*, 1975; *Nummedal et al.*, 1984] is indicated by evidence of a relict shoreline, similar to height drowning in our model. Transgressive submergence predicts the generation of shelf sand bodies without preservation of shoreline sands [*Penland et al.*, 1988] and might be comparable to width drowning in our model. Additionally, *Orford et al.* [2010] identify "functional breakdown" when the protection of barrier height against flooding is lost, which could correspond to height drowning in our model, and "geomorphological breakdown" when the barrier ceases to act as a coherent assemblage of coarse sediment, akin to width drowning in our model.

7.4. Model Limitations and Future Work

The model results presented here are not aimed at specifically reproducing the evolution of any particular barrier system. Instead, we focus on the long-term coupling between shoreface dynamics and overwash processes, which requires leaving out other processes that could affect barrier evolution. For instance, we assume that the barrier is composed by uniform-grain and noncohesive sediment. Also, along many coasts, nonsandy lithology outcrops at the shore (or just offshore), playing a poorly understood role in the changes occurring at the shoreline itself [*Thieler et al.*, 2000; *Pilkey and Cooper*, 2004; *Valvo et al.*, 2006; *Cooper et al.*, 2012]. However, the parameter space explorations could allow for deeper interpretation of the influence of framework geology. For example, a "perched" barrier atop harder lithology would have a forced shallow shoreface and therefore high shoreface response rate K. Shorefaces with access to deeper reservoirs of sandy sediment would correspondingly have a potentially longer response timescale and lower representative values for K.

Additionally, the model only considers sediment transport in the cross-shore direction. Although barrier drowning is locally a cross-shore problem, previous studies of cross-shore sediment transport indicate that even small gradients in alongshore sediment flux can overwhelm profile changes [*Cowell et al.*, 1995; *McNinch et al.*, 1999; *Thieler et al.*, 2000]. The model also does not consider the effect of individual events, assuming the existence of a constant frequency "characteristic event" responsible for controlling the morphological change in the barrier system. In this way, we are basically replacing the time series of storm events with an average rate of storm overwash. Additionally, the model does not include any process that could fill the back-barrier lagoon with sediments (e.g., fluvial, estuarine, and/or marsh sedimentation). Consequently, the depths of the back-barrier lagoon in the model are generally large compared to many real barrier systems.

Leaving out many of the processes operating in a complex system such as a barrier island can potentially increase the clarity and insights the model facilitates [*Murray*, 2003]. In our case, simplification of the system has been successful at capturing the long-term coupling between shoreface evolution and overwash processes. Moreover, given the striking simplicity of the model, it can be easily adjusted to explore other key

processes that might affect barrier evolution, including the ones mentioned above. For instance, motivated by the model results that suggest that barrier evolution can be very sensitive to changes in the back-barrier lagoon slope (Figure 12), the model could easily explore more complex back-barrier environment configurations, including, for example, changes in estuarine and/or marsh sedimentation. Also, given the simplicity of the cross-shore model, extending the model through many profiles coupled by alongshore sediment transport [*Ashton and Murray*, 2006] will be numerically efficient. Finally, future versions of the model will be extended to account for temporal changes in the frequency and the magnitude of storms and therefore will separate between storm events and "calm weather."

8. Conclusions

We have constructed a simple morphodynamic model for the long-term evolution of coastal barriers. Barrier evolution in the model is driven by sea-level rise, storm overwash, and a dynamic shoreface. The model involves a coupled system of four ordinary differential equations, which represents a significant simplification respect to current morphodynamic models [*Storms et al.*, 2002; *Masetti et al.*, 2008; *Ashton and Ortiz*, 2011]. The model demonstrates that internal barrier system dynamics can lead to previously unidentified complex barrier responses. The model can attain dynamic equilibrium, matching the rollover state in which the barrier attains a fixed geometry as it migrates landward. However, barriers may also drown, either vertically if the overwash flux is insufficient to maintain the subaqueous portion of the barrier or horizontally if the shoreface response is insufficient to maintain the barrier geometry during landward migration. Furthermore, the model predicts that the barrier system can experience periodic retreat, even with constant sea-level rise rate, due to time lags in the shoreface response to barrier overwash. This periodic behavior demonstrates the potential for threshold behavior, whereby a slowly evolving, seemingly steady barrier system can undergo abrupt rapid increases in retreat rate (which can also be followed by periods of prolonged slow evolution).

By exploring barrier evolution across a wide swath of parameter space, the model predicts that barrier drowning, and in particular width drowning, will become a much more common barrier process for higher sea-level rise rates (Figure 15). Overall, the model results highlight the importance of using a morphodynamic approach to understand the dynamics of coastal systems.

Acknowledgments
This research has been supported by the National Science Foundation grant #CNH-0815875, the Strategic Environment Research and Development Program, and the Coastal Ocean Institute of the Woods Hole Oceanographic Institution. We thank Rob Evans, Jeff Donnelly, and Alejandra Ortiz for fruitful discussions.

References

Ashton, A., and A. B. Murray (2006), High-angle wave instability and emergent shoreline shapes: 1. Modeling of sand waves, flying spits, and capes, *J. Geophys. Res.*, *111*, F04011, doi:10.1029/2005JF000422.

Ashton, A. D., and A. C. Ortiz (2011), *Overwash Control Coastal Barrier Response to Sea-Level Rise*, Coastal Sediments '11, pp. 230–243, World Scientific, Miami, Florida.

Bailard, J. A. (1981), An energetics total load sediment transport model for a plane sloping beach, *J. Geophys. Res.*, *86*, 10,938–910,954.

Beets, D. J., and A. Van der Spek (2000), The Holocene evolution of the barrier and back-barrier basins of Belgium and the Netherlands as a function of late Weichselian morphology, relative sea-level rise and sediment supply, *Geol. Mijnbouw*, *79*(1), 3–16.

Bowen, A. J. (1980), Simple models of nearshore sedimentation: Beach profiles and longshore bars, in *The Coastline of Canada*, edited by S. B. McCann, pp. 1–11, Geological Survey of Canada, Ottawa, Ontario.

Bruun, P. (1962), Sea-level rise as a cause of shore erosion, *Proc. ASCE J. Waterways Harbors Div.*, *88*, 117–130.

Bruun, P. (1988), The Bruun rule of erosion: A discussion on large-scale two and three dimensional usage, *J. Coastal Res.*, *4*, 626–648.

Carruthers, E. A., D. P. Lane, R. L. Evans, J. P. Donnelly, and A. D. Ashton (2013), Quantifying overwash flux in barrier systems: An example from Martha's Vineyard, Massachusetts, USA, *Mar. Geol.*, *343*, 15–28.

Clifton, H. (2006), A reexamination of facies models for clastic shorelines, *SEPM Spetial Publ.*, *84*, 293.

Cooper, J., D. Jackson, A. Dawson, S. Dawson, C. Bates, and W. Ritchie (2012), Barrier islands on bedrock: A new landform type demonstrating the role of antecedent topography on barrier form and evolution, *Geology*, *40*(10), 923–926.

Cowell, P. J., P. S. Roy, and R. A. Jones (1995), Simulation of large-scale coastal change using a morphological behavior model, *Mar. Geol.*, *126*(1–4), 45–61.

Daley, M., and P. J. Cowell (2012), Long-term shoreface response to disequilibrium-stress: A conundrum for climate change, *21st NSW Coastal Conference*.

De Beaumont, L. E. (1845), Leçons de géologie pratique: Professées au Collége de France, *pendant l'année scolaire 1843-1844*, P. Bertrand.

Dean, R. G. (1991), Equilibrium Beach Profiles: Characteristics and Applications, *J. Coastal Res.*, *7*(1), 53–84.

Dean, R. G., and E. M. Maurmeyer (1983), Models for beach profile response, in *Handbook of Coastal Processes and Erosion*, edited by P. D. Komar, pp. 151–165, CRC Press, Boca Raton, Florida, USA.

Dillon, W. P. (1970), Submergence effects on a Rhode island barrier and lagoon and inferences on migration of barriers, *J. Geol.*, *78*(1), 94–106.

Donnelly, C., N. Kraus, and M. Larson (2006), State of Knowledge on Measurement and Modeling of Coastal Overwash, *J. Coastal Res.*, *22*(4), 965–991.

Engelhart, S. E., B. P. Horton, B. C. Douglas, W. R. Peltier, and T. E. Tornqvist (2009), Spatial variability of late Holocene and 20(th) century sea-level rise along the Atlantic coast of the United States, *Geology*, *37*(12), 1115–1118.

Fagherazzi, S., P. W. Wiberg, and A. D. Howard (2003), *Modeling barrier island formation and evolution, paper presented at Proceedings of the International Conference on Coastal Sediments 2003*, CD-ROM Published by, World Scientific Publishing Corp. and East Meets West Productions, Corpus Christi, Texas, USA., St. Petersburg, Florida.

Falqués, A., F. Ribas, P. Larroude, and A. Montoto (1999), Nearshore oblique bars. Modelling versus observations at the Truc Vert Beach, paper presented at I. A. H. R. Symposium on River, Coastal and Estuarine Morphodynamics, DIAM, Genoa, Italy.
Fitzgerald, D. M., S. Penland, and D. Nummedal (1984), Control of barrier island shape by inlet sediment bypassing: East Frisian Islands, West Germany, *Mar. Geol.*, *60*(1–4), 355–376.
FitzGerald, D. M., M. S. Fenster, B. A. Argow, and I. V. Buynevich (2008), Coastal impacts due to sea-level rise, in *Annu. Rev. Earth Planet. Sci*, pp. 601–647, Annual Reviews, Palo Alto.
Forbes, D. L., R. B. Taylor, J. D. Orford, R. W. G. Carter, and J. Shaw (1991), Gravel-barrier migration and overstepping, *Mar. Geol.*, *97*(3–4), 305–313.
Gilbert, G. K. (1885), The topographic features of lake shores, *U. S. Geol. Surv. Annu. Rep.*, *5*, 69–123.
González, F. I., V. V. Titov, H. O. Mofjeld, A. J. Venturato, R. S. Simmons, R. Hansen, R. Combellick, R. K. Eisner, D. F. Hoirup, and B. S. Yanagi (2005), Progress in NTHMP hazard assessment, *Nat. Hazards*, *35*(1), 89–110.
Gutierrez, B. T., N. G. Plant, and E. R. Thieler (2011), A Bayesian network to predict coastal vulnerability to sea level rise, *J. Geophys. Res.*, *116*, F02009, doi:10.1029/2010JF001891.
Hallermeier, R. J. (1981), A profile zonation for seasonal sand beaches from wave climate, *Coast Eng.*, *4*, 253–277.
Hawkes, A. D., and B. P. Horton (2012), Sedimentary record of storm deposits from Hurricane Ike, Galveston and San Luis Islands, Texas, *Geomorphology*, *171*, 180–189.
Heward, A. P. (1981), A review of wave-dominated clastic shoreline deposits, *Earth Sci. Rev.*, *17*(3), 223–276.
Hoyt, J. H., and V. J. Henry (1971), Origin of capes and shoals along the southeastern coast of the United States, *GSA Bull.*, *82*, 59–66.
IPCC, I. P. o. C. C (2007), *Climate Change 2007: The Physical Science Basis*, Cambridge Univ. Press, New York.
Jiménez, J., and A. Sánchez-Arcilla (2004), A long-term (decadal scale) evolution model for microtidal barrier systems, *Coast Eng.*, *51*(8–9), 749–764.
Kim, W., and T. Muto (2007), Autogenic response of alluvial-bedrock transition to base-level variation: Experiment and theory, *J. Geophys. Res.*, *112*, F03S14, doi:10.1029/2006JF000561.
Larson, M., and N. C. Kraus (1989), SBEACH: Numerical model for simulating storm-induced beach change; Report 1, Empirical foundation and model development, in *Technical Report CERC-89-9*, U.S. Army Engineer Waterways Experiment Station, Coastal Engineering Research Center, Vicksburg, MS, 1–115.
Larson, M., L. Erikson, and H. Hanson (2004), An analytical model to predict dune erosion due to wave impact, *Coast Eng.*, *51*(8–9), 675–696.
Leatherman, S. P. (1979), Migration of Assateague Island, Maryland, by inlet and overwash processes, *Geology*, *7*, 104–107.
Leatherman, S. P. (1983), Barrier dynamics and landward migration with Holocene sea-level rise, *Nature*, *301*(3 February), 415–417.
Lindemer, C. A., N. G. Plant, J. A. Puleo, D. M. Thompson, and T. V. Wamsley (2010), Numerical simulation of a low-lying barrier island's morphological response to Hurricane Katrina, *Coast Eng.*, *57*(11–12), 985–995.
Lorenzo-Trueba, J., and V. R. Voller (2010), Analytical and numerical solution of a generalized Stefan problem exhibiting two moving boundaries with application to ocean delta formation, *J. Math. Anal. Appl.*, *366*(2), 538–549.
Lorenzo-Trueba, J., V. R. Voller, T. Muto, W. Kim, C. Paola, and J. B. Swenson (2009), A similarity solution for a dual moving boundary problem associated with a coastal-plain depositional system, *J. Fluid Mech.*, *628*, 427–443.
Lorenzo-Trueba, J., V. R. Voller, C. Paola, R. R. Twilley, and A. E. Bevington (2012), Exploring the role of organic matter accumulation on delta evolution, *J. Geophys. Res.*, *117*, F00A02, doi:10.1029/2012JF002339.
Lorenzo-Trueba, J., V. R. Voller, and C. Paola (2013), A geometric model for the dynamics of a fluvially dominated deltaic system under base-level change, *Comp. Geosci.*, *53*, 39–47.
Masetti, R., S. Fagherazzi, and A. Montanari (2008), Application of a barrier island translation model to the millennial-scale evolution of Sand Key, Florida, *Cont. Shelf Res.*, *28*(9), 1116–1126.
McBride, R. A., et al. (2013), Morphodynamics of barrier systems: A synthesis, in *Treatise on Geomorphology*, edited by J. E. i. C. Shroder and D. Sherman, pp. 166–244, Academic Press, San Diego, Calif.
McCall, R. T., J. S. M. Van Thiel de Vries, N. G. Plant, A. R. Van Dongeren, J. A. Roelvink, D. M. Thompson, and A. J. H. M. Reniers (2010), Two-dimensional time dependent hurricane overwash and erosion modeling at Santa Rosa Island, *Coast Eng.*, *57*(7), 668–683.
McGee, W. J. (1891), *The Lafayette Formation, 12th Ann. Rept. 1890–91*, pp. 347–521, U.S. Geol. Surv., Washington.
McNamara, D. E., and B. T. Werner (2008), Coupled barrier island-resort model: 1. Emergent instabilities induced by strong human-landscape interactions, *J. Geophys. Res.*, *113*, F01016, doi:10.1029/2007JF000840.
McNinch, J. E., J. T. Wells, and S. W. Snyder (1999), The long-term contribution of pre-holocene sands to transgressing barrier islands, paper presented at Coastal Sediments '99, ASCE, Long Island.
Mellett, C. L., D. M. Hodgson, A. Lang, B. Mauz, I. Selby, and A. J. Plater (2012), Preservation of a drowned gravel barrier complex: A landscape evolution study from the north-eastern English Channel, *Mar. Geol.*, *315–318*, 115–131.
Miller, J. K., and R. G. Dean (2004), A simple new shoreline change model, *Coast Eng.*, *51*(7), 531–556.
Moore, L. J., J. H. List, S. J. Williams, and D. Stolper (2010), Complexities in barrier island response to sea level rise: Insights from numerical model experiments, North Carolina Outer Banks, *J. Geophys. Res.*, *115*, F03004, doi:10.1029/2009JF001299.
Murray, A. B. (2003), Contrasting the goals, strategies, and predictions associated with simplified numerical models and detailed simulations, in *Prediction in Geomorphology, AGU Geophysical Monograph 135*, edited by R. M. Iverson and P. R. Wilcock, pp. 151–165, AGU, Washington, D. C.
Nicholls, R. J., W. A. Birkemeier, and G. H. Lee (1998), Evaluation of depth of closure using data from Duck, NC, USA, *Mar. Geol.*, *148*(3–4), 179–201.
Nummedal, D., R. Cuomo, and B. Kofron (1984), In-place barrier drowning on Louisiana Continental Shelf, *Am. Assoc. Pet. Geol., Bull.;(United States)*, *68*(CONF-8405216-).
Orford, J., S. Jennings, and J. Pethick (2010), Extreme storm effect on gravel-dominated barriers.
Ortiz, A. C., and A. Ashton (2013), A Morphodynamic Explanation for the Shoreface Depth of Closure, *8th Symposium on River, Coastal and Estuarine Morphodynamics*.
Otvos, E. G. (1985), Barrier Island Genesis-Questions of Alternatives for the Apalachicola Coast, Northeastern Gulf of Mexico, *J. Coastal Res.*, *1*(3), 267–291.
Penland, S., R. Boyd, and J. R. Suter (1988), Transgressive depositional systems of the Mississippi Delta plain - A model for barrier shoreline and shelf sand development, *J. Sediment. Petrol.*, *58*(6), 932–949.
Pierce, J. W. (1970), Tidal inlets and washover fans, *J. Geol.*, *78*, 230–234.
Pilkey, O. H., and J. A. G. Cooper (2004), CLIMATE: Society and sea level rise, *Science*, *303*(5665), 1781–1782, doi:10.1126/science.1093515.
Plant, N. G., and H. F. Stockdon (2012), Probabilistic prediction of barrier-island response to hurricanes, *J. Geophys. Res.*, *117*, F03015, doi:10.1029/2011JF002326.

Rahmstorf, S., G. Foster, and A. Cazenave (2012), Comparing climate projections to observations up to 2011, *Environ. Res. Lett.*, *7*(4), 044035.
Rampino, M. R., and J. E. Sanders (1980), Holocene transgression in south-central long-island, New York, *J. Sediment. Petrol.*, *50*(4), 1063–1080.
Ranasinghe, R., and M. F. Stive (2009), Rising seas and retreating coastlines, *Clim. Change*, *97*(3–4), 465–468.
Ranasinghe, R., D. Callaghan, and M. F. Stive (2012), Estimating coastal recession due to sea level rise: Beyond the Bruun rule, *Clim. Change*, *110*(3–4), 561–574.
Reinson, G. E. (1979), Facies Models 14. Barrier Island Systems.
Rodriguez, A. B., J. B. Anderson, F. P. Siringan, and M. Taviani (2004), Holocene evolution of the east Texas coast and inner continental shelf: Along-strike variability in coastal retreat rates, *J. Sediment. Res.*, *74*(3), 405–421.
Roelvink, D., A. Reniers, A. van Dongeren, J. van Thiel de Vries, R. McCall, and J. Lescinski (2009), Modelling storm impacts on beaches, dunes and barrier islands, *Coast Eng.*, *56*(11–12), 1133–1152.
Roelvink, J. A. (2006), Coastal morphodynamic evolution techniques, *Coast Eng.*, *53*(2–3), 277–287.
Rosati, J. D., R. G. Dean, and G. W. Stone (2010), A cross-shore model of barrier island migration over a compressible substrate, *Mar. Geol.*, *271*(1–2), 1–16.
Sanders, J. E., and N. Kumar (1975), Evidence of shoreface retreat and in-place "drowning" during Holocene submergence of barriers, shelf off Fire Island, New York, *Geol. Soc. Am. Bull.*, *86*(1), 65–76.
Scheinerman, E. R. (1996), *Invitation to dynamical systems*, 373 pp., Prentice Hall, Upper Saddle River, N. J.
Smith, M. D., J. M. Slott, D. McNamara, and A. Brad Murray (2009), Beach nourishment as a dynamic capital accumulation problem, *J. Environ. Econ. Manage.*, *58*(1), 58–71.
Stahl, L., J. Koczan, and D. Swift (1974), Anatomy of a Shoreface-Connected Sand Ridge on the New Jersey Shelf: Implications for the Genesis of the Shelf Surficial Sand Sheet, *Geology*, *2*(3), 117–120.
Stive, M. J. F., and H. J. de Vriend (1995), Modelling shoreface profile evolution, *Mar. Geol.*, *126*(1–4), 235–248.
Stive, M. J. F., R. J. Nicholls, and H. J. deVriend (1991), Sea-level rise and shore nourishment - a discussion, *Coast Eng.*, *16*(1), 147–163.
Stive, M. J. F., S. G. J. Aarninkhof, L. Hamm, H. Hanson, M. Larson, K. M. Wijnberg, R. J. Nicholls, and M. Capobianco (2002), Variability of shore and shoreline evolution, *Coast Eng.*, *47*(2), 211–235.
Stolper, D., J. H. List, and E. R. Thieler (2005), Simulating the evolution of coastal morphology and stratigraphy with a new morphological-behaviour model (GEOMBEST), *Mar. Geol.*, *218*(1–4), 17–36.
Stone, G. W., and R. A. McBride (1998), Louisiana Barrier Islands and Their Importance in Wetland Protection: Forecasting Shoreline Change and Subsequent Response of Wave Climate, *J. Coastal Res.*, *14*(3), 900–915.
Storms, J. E. A. (2003), Event-based stratigraphic simulation of wave-dominated shallow-marine environments, *Mar. Geol.*, *199*(1–2), 83–100.
Storms, J. E. A., and D. J. P. Swift (2003), Shallow-marine sequences as the building blocks of stratigraphy: Insights from numerical modelling, *Basin Res.*, *15*(3), 287–303.
Storms, J. E. A., and G. J. Hampson (2005), Mechanisms for forming discontinuity surfaces within shoreface-shelf parasequences: Sea level, sediment supply, or wave regime?, *J. Sediment. Res.*, *75*(1), 67–81.
Storms, J. E. A., G. J. Weltje, J. J. Van Dijke, C. R. Geel, and S. B. Kroonenberg (2002), Process-response modeling of wave-dominated coastal systems: Simulating evolution and stratigraphy on geological timescales, *J. Sediment. Res.*, *72*(2), 226–239.
Storms, J. E. A., G. J. Weltje, G. J. Terra, A. Cattaneo, and F. Trincardi (2008), Coastal dynamics under conditions of rapid sea-level rise: Late Pleistocene to Early Holocene evolution of barrier-lagoon systems on the northern Adriatic shelf (Italy), *Quat. Sci. Rev.*, *27*(11–12), 1107–1123.
Stuiver, M., and J. J. Daddario (1963), Submergence of the New Jersey Coast, *Science*, *142*(3594), 951.
Stutz, M. L., and O. H. Pilkey (2001), A Review of Global Barrier Island Distribution, *J. Coastal Res.*, *34*, 15–22.
Stutz, M. L., and O. H. Pilkey (2011), Open-Ocean Barrier Islands: Global Influence of Climatic, Oceanographic, and Depositional Settings, *J. Coastal Res.*, *27*(2), 207–222.
Swenson, J. B., V. R. Voller, C. Paola, G. Parker, and J. G. Marr (2000), Fluvio-deltaic sedimentation: A generalized Stefan problem, *Euro*, *J. Appl. Math.*, *11*, 433–452.
Swift, D. J. P. (1975), Barrier-island genesis: Evidence from the central atlantic shelf, eastern U.S.A, *Sediment. Geol.*, *14*(1), 1–43.
Swift, D. J. P., and T. F. Moslow (1982), Holocene transgression in South Central Long Island, New York - Discussion, *J. Sediment. Petrol.*, *52*(3), 1014–1019.
Thieler, E. R., and A. D. Ashton (2011), 'Cape capture': Geologic data and modeling results suggest the Holocene loss of a Carolina Cape, *Geology*, *39*(4), 339–342.
Thieler, E. R., O. H. Pilkey Jr., R. S. Young, D. M. Bush, and F. Chai (2000), The Use of Mathematical Models to Predict Beach Behavior for U.S. Coastal Engineering: A Critical Review, *J. Coastal Res.*, *16*(1), 48–70.
Valdemoro, H. I., A. Sanchez-Arcilla, and J. A. Jiménez (2007), Coastal dynamics and watlands stability. The Ebro Delta case, *Hydrobiologia*, *577*, 17–29, doi:10.1007/s10750-10006-041407.
Valvo, L. M., A. B. Murray, and A. D. Ashton (2006), How does underlying geology affect coastline change? An initial modeling investigation, *J. Geophys. Res.*, *111*, F02025, doi:10.1029/2005JF000340.
Wolinsky, M. A., and A. B. Murray (2009), A unifying framework for shoreline migration: 2. Application to wave-dominated coasts, *J. Geophys. Res.*, *114*, F01009, doi:10.1029/2007JF000856.
Wright, L. D. (1995), *Morphodynamics of inner continental shelves*, 241 pp., CRC Press, Boca Raton.
Wright, L. D., J. D. Boon, S. C. Kim, and J. H. List (1991), Modes of cross-shore sediment transport on the shoreface of the Middle Atlantic Bight, *Mar. Geol.*, *96*(1–2), 19–51.
Yates, M. L., R. T. Guza, and W. C. O'Reilly (2009), Equilibrium shoreline response: Observations and modeling, *J. Geophys. Res.*, *114*, C09014, doi:10.1029/2009JC005359.